

Research Summary

N. Venkovic
nvenkov1@jhu.edu

Supervisor: Prof. L. Graham-Brady
lori@jhu.edu

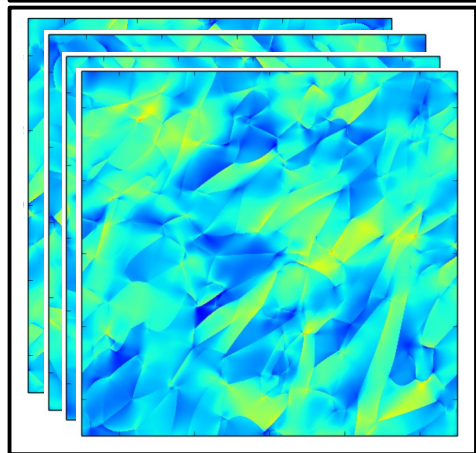


Group Meeting
October 4, 2017

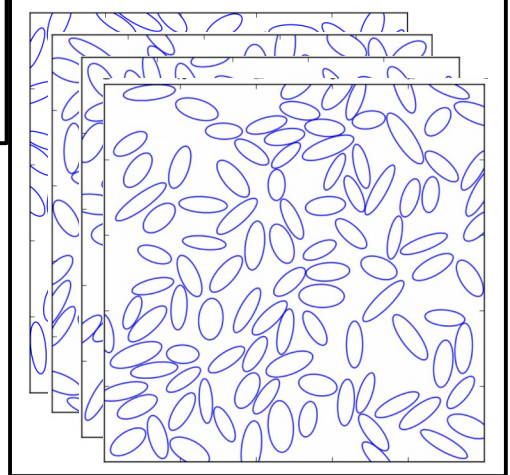
Motivation/Objective

- Understand the role of morphology on the mechanical performance of random polycrystals

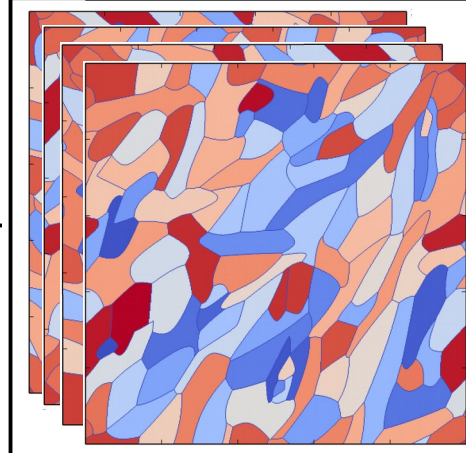
Full-field simulation of elastic and elasto-viscoplastic behaviors



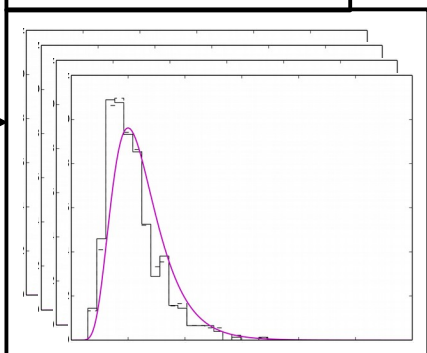
Simulation of
Markov marked
point processes



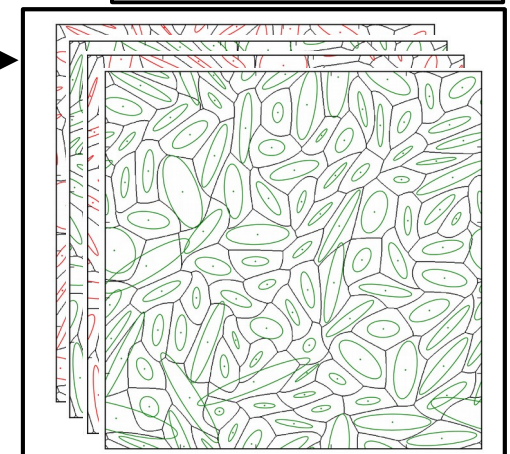
Ellipsoidal Growth
Tessellations



Field-statistics



Morphological
characterization



Explore a potentially
more efficient and
insightful way

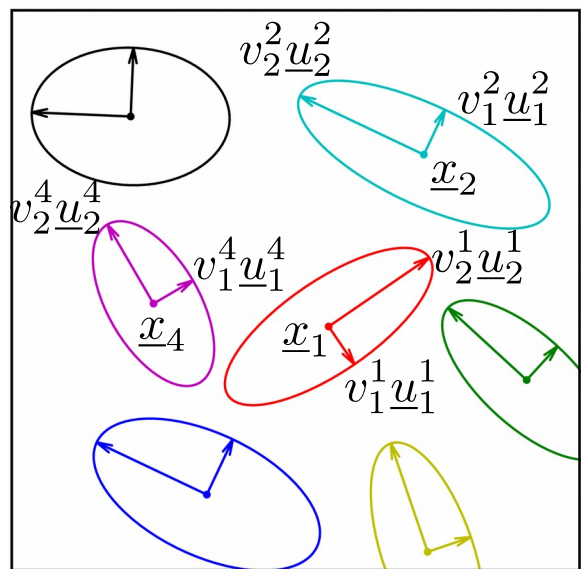
Ellipsoidal growth structures (EGS)

Ellipsoidal growth structures (EGS) are morphological models defined with marked point patterns (MPP). Underlying microstructures are constructed after a rule invoking the MPP.

Example: Tessellations.

- MPP: $\{(\underline{x}_\alpha, \mathbf{Z}_\alpha)\}$
- Rule: $\Omega_\alpha = \{\underline{x} \mid \underset{\gamma}{\operatorname{argmin}} (\underline{x} - \underline{x}_\gamma) \cdot \mathbf{Z}_\gamma \cdot (\underline{x} - \underline{x}_\gamma) = \alpha\}$

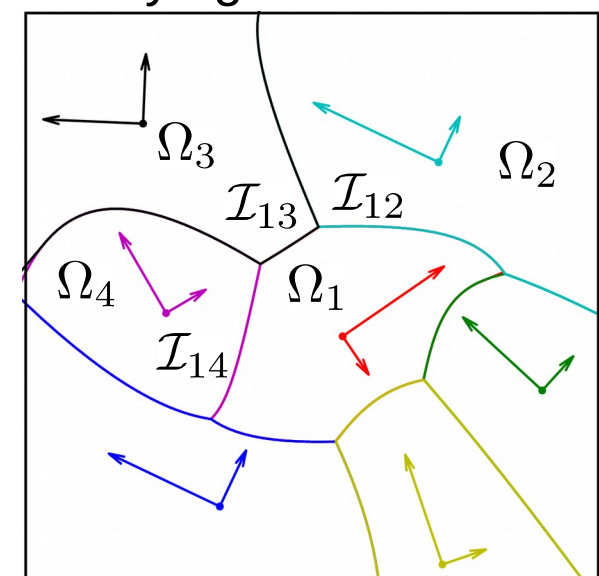
MPP



$$\mathbf{Z}_\alpha = \frac{\underline{u}_1^\alpha \otimes \underline{u}_1^\alpha}{(v_1^\alpha)^2} + \frac{\underline{u}_2^\alpha \otimes \underline{u}_2^\alpha}{(v_2^\alpha)^2}$$

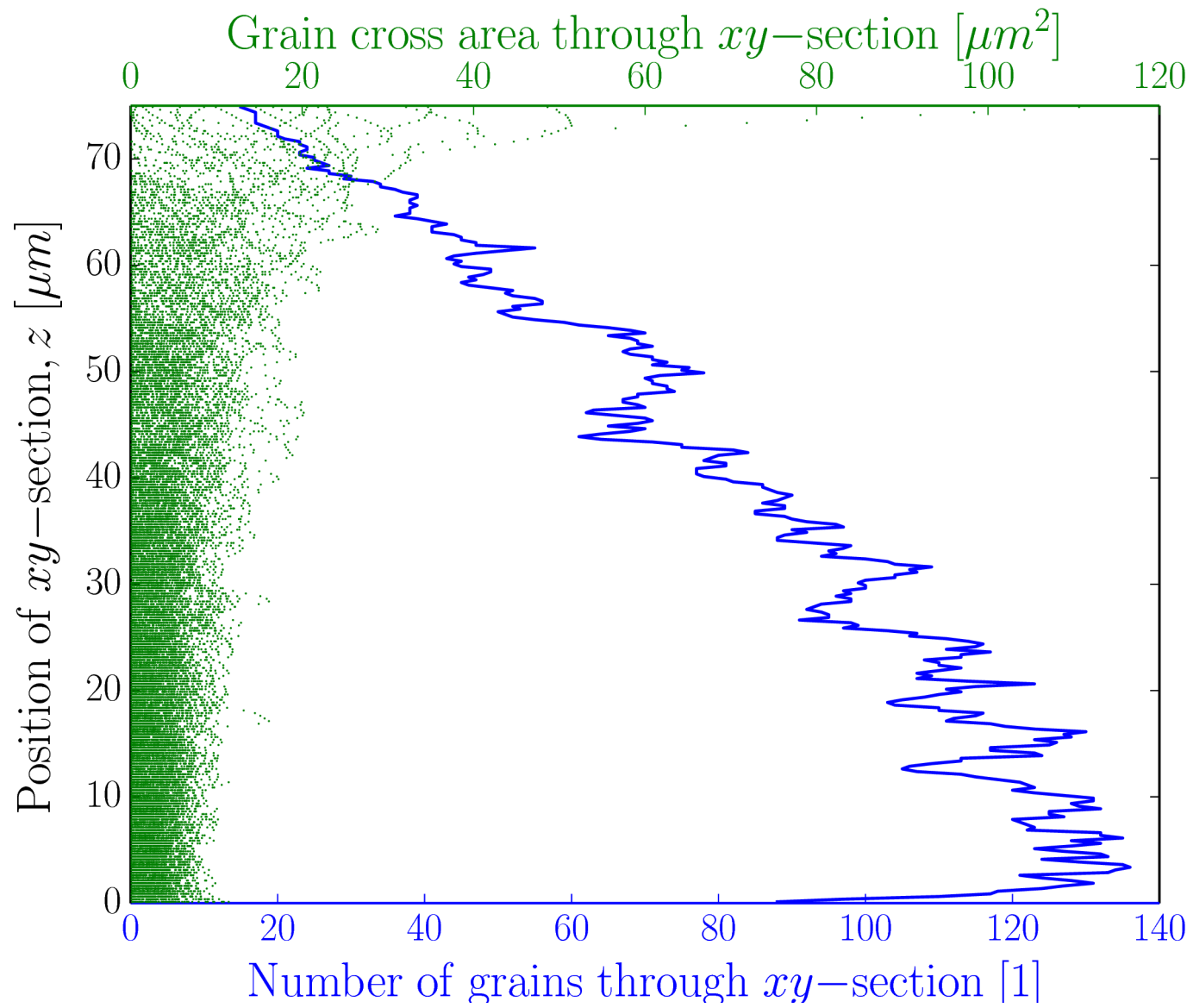
Resolution

Underlying microstructure



Every cell Ω_α with boundary $\partial\Omega_\alpha$ can be reconstructed from common curves $\mathcal{I}_{\alpha\gamma}$. Can we solve for $\mathcal{I}_{\alpha\gamma}$?

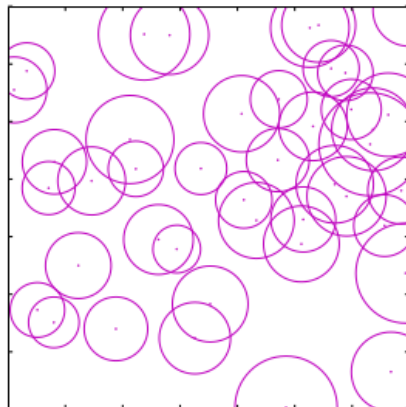
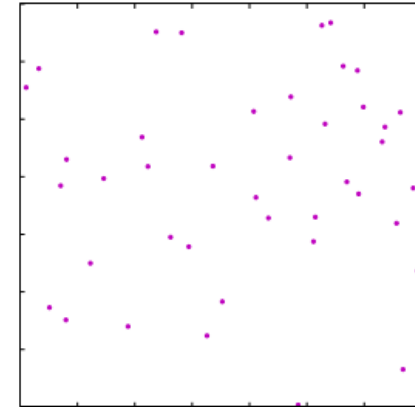
EGS – Simulation



MPP simulation by collective rearrangement

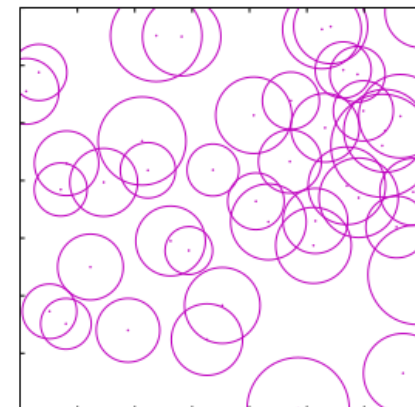
Simulation of the point process

Simulate the point set $\{\vec{x}_{i,0} \mid i = 1, N\}$ in the container of size A_{cont} after a Poisson point process with rate $\lambda = 1/\mathbb{E}[A]$.



Simulation of the marks

Simulate the mark set $\{r_{i,0} \mid i = 1, N\}$ independently of the points after the prescribed grain distribution $f_A(a)$ and where $r = \sqrt{a/\pi}$.



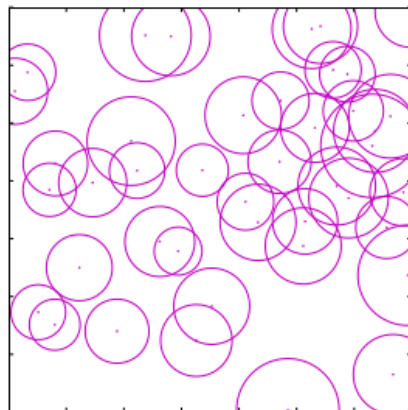
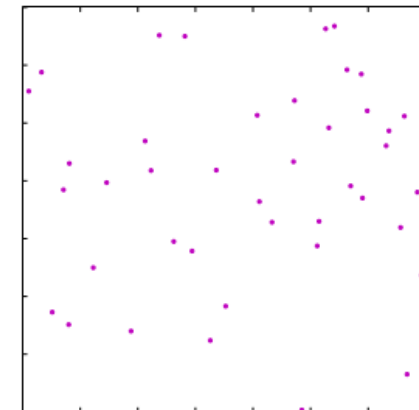
Rearrangement of the marked point set

Assuming a pair potential p_{ij} between arbitrary marked points $(\vec{x}_i; r_i)$ and $(\vec{x}_j; r_j)$, modify the marked point set using the force-biased algorithm.

MPP simulation by collective rearrangement

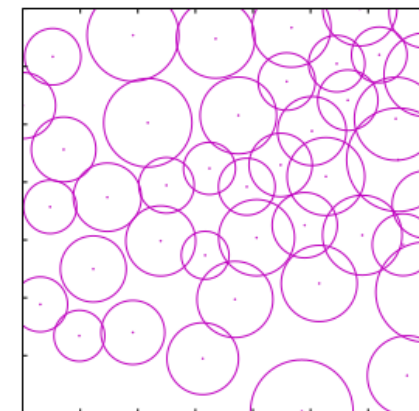
Simulation of the point process

Simulate the point set $\{\vec{x}_{i,0} \mid i = 1, N\}$ in the container of size A_{cont} after a Poisson point process with rate $\lambda = 1/\mathbb{E}[A]$.



Simulation of the marks

Simulate the mark set $\{r_{i,0} \mid i = 1, N\}$ independently of the points after the prescribed grain distribution $f_A(a)$ and where $r = \sqrt{a/\pi}$.



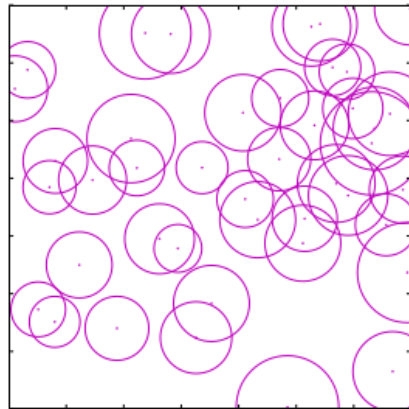
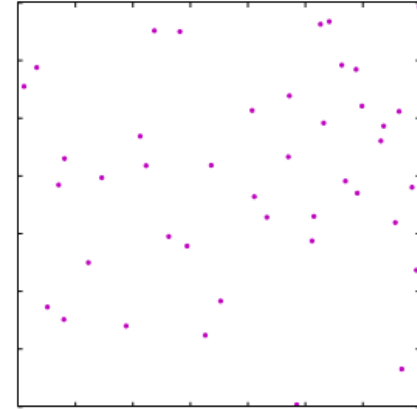
Rearrangement of the marked point set

Assuming a pair potential p_{ij} between arbitrary marked points $(\vec{x}_i; r_i)$ and $(\vec{x}_j; r_j)$, modify the marked point set using the force-biased algorithm.

MPP simulation by collective rearrangement

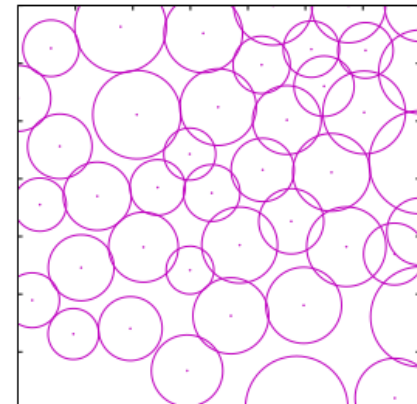
Simulation of the point process

Simulate the point set $\{\vec{x}_{i,0} \mid i = 1, N\}$ in the container of size A_{cont} after a Poisson point process with rate $\lambda = 1/\mathbb{E}[A]$.



Simulation of the marks

Simulate the mark set $\{r_{i,0} \mid i = 1, N\}$ independently of the points after the prescribed grain distribution $f_A(a)$ and where $r = \sqrt{a/\pi}$.



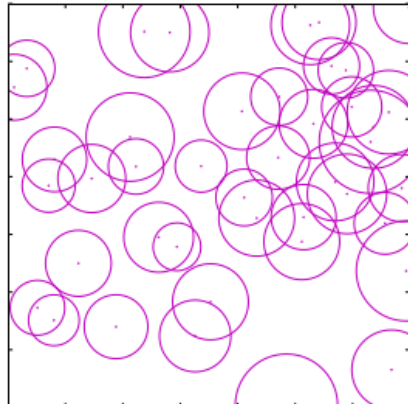
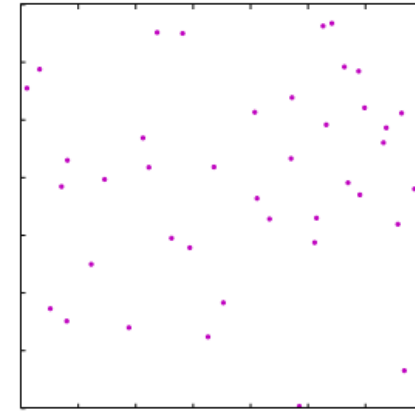
Rearrangement of the marked point set

Assuming a pair potential p_{ij} between arbitrary marked points $(\vec{x}_i; r_i)$ and $(\vec{x}_j; r_j)$, modify the marked point set using the force-biased algorithm.

MPP simulation by collective rearrangement

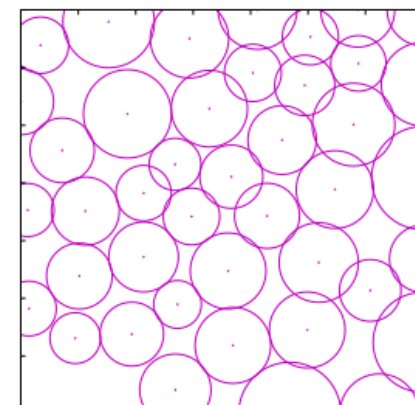
Simulation of the point process

Simulate the point set $\{\vec{x}_{i,0} \mid i = 1, N\}$ in the container of size A_{cont} after a Poisson point process with rate $\lambda = 1/\mathbb{E}[A]$.



Simulation of the marks

Simulate the mark set $\{r_{i,0} \mid i = 1, N\}$ independently of the points after the prescribed grain distribution $f_A(a)$ and where $r = \sqrt{a/\pi}$.



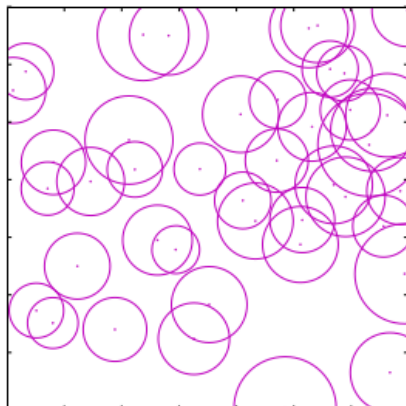
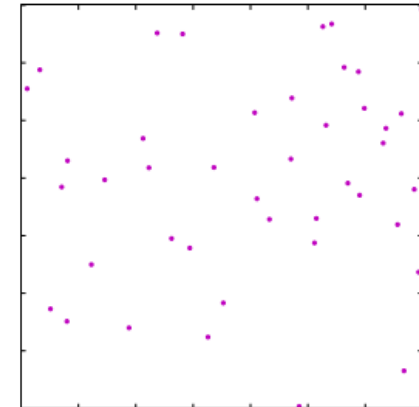
Rearrangement of the marked point set

Assuming a pair potential p_{ij} between arbitrary marked points $(\vec{x}_i; r_i)$ and $(\vec{x}_j; r_j)$, modify the marked point set using the force-biased algorithm.

MPP simulation by collective rearrangement

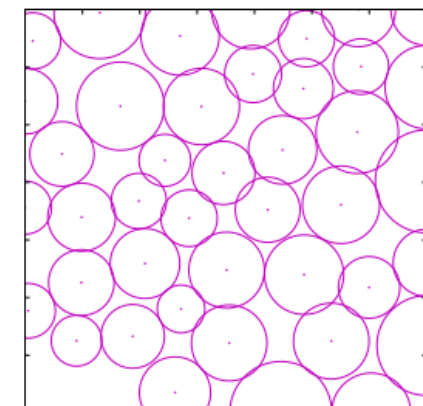
Simulation of the point process

Simulate the point set $\{\vec{x}_{i,0} \mid i = 1, N\}$ in the container of size A_{cont} after a Poisson point process with rate $\lambda = 1/\mathbb{E}[A]$.



Simulation of the marks

Simulate the mark set $\{r_{i,0} \mid i = 1, N\}$ independently of the points after the prescribed grain distribution $f_A(a)$ and where $r = \sqrt{a/\pi}$.



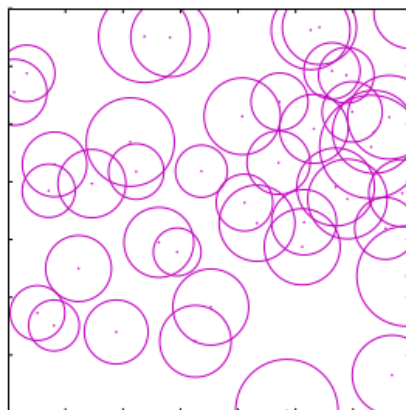
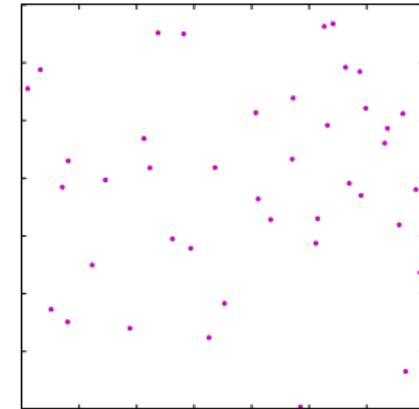
Rearrangement of the marked point set

Assuming a pair potential p_{ij} between arbitrary marked points $(\vec{x}_i; r_i)$ and $(\vec{x}_j; r_j)$, modify the marked point set using the force-biased algorithm.

MPP simulation by collective rearrangement

Simulation of the point process

Simulate the point set $\{\vec{x}_{i,0} \mid i = 1, N\}$ in the container of size A_{cont} after a Poisson point process with rate $\lambda = 1/\mathbb{E}[A]$.

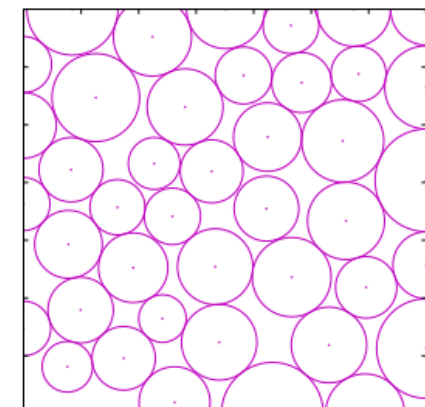


Simulation of the marks

Simulate the mark set $\{r_{i,0} \mid i = 1, N\}$ independently of the points after the prescribed grain distribution $f_A(a)$ and where $r = \sqrt{a/\pi}$.

Rearrangement of the marked point set

Assuming a pair potential p_{ij} between arbitrary marked points $(\vec{x}_i; r_i)$ and $(\vec{x}_j; r_j)$, modify the marked point set using the force-biased algorithm.



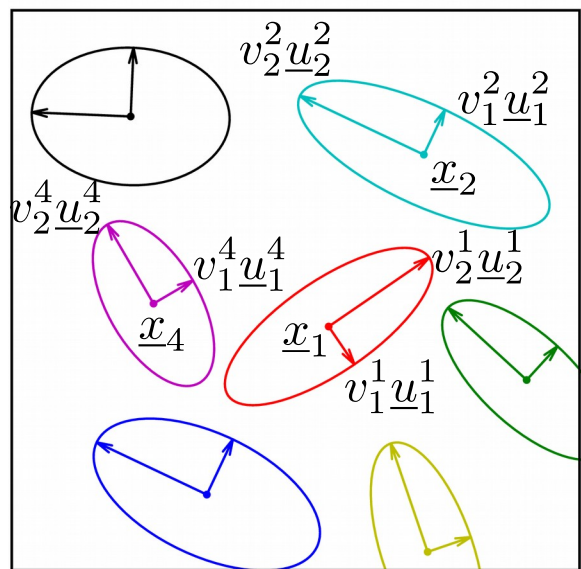
Ellipsoidal growth structures (EGS)

Ellipsoidal growth structures (EGS) are morphological models defined with marked point patterns (MPP). Underlying microstructures are constructed after a rule invoking the MPP.

Example: Tessellations.

- MPP: $\{(\underline{x}_\alpha, \mathbf{Z}_\alpha)\}$
- Rule: $\Omega_\alpha = \{\underline{x} \mid \underset{\gamma}{\operatorname{argmin}} (\underline{x} - \underline{x}_\gamma) \cdot \mathbf{Z}_\gamma \cdot (\underline{x} - \underline{x}_\gamma) = \alpha\}$

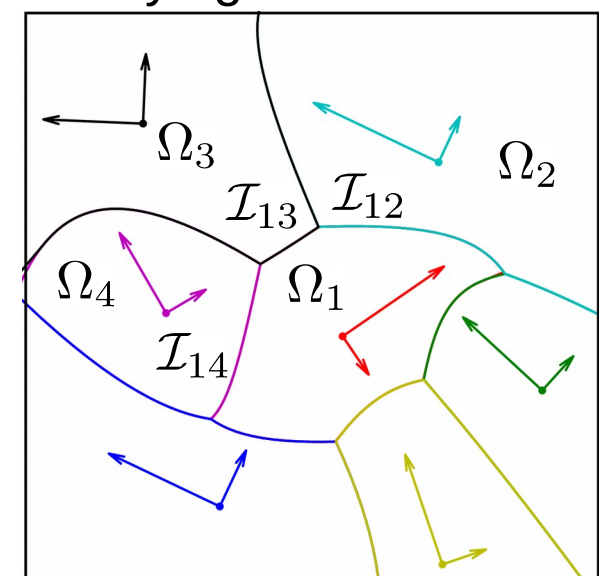
MPP



$$\mathbf{Z}_\alpha = \frac{\underline{u}_1^\alpha \otimes \underline{u}_1^\alpha}{(v_1^\alpha)^2} + \frac{\underline{u}_2^\alpha \otimes \underline{u}_2^\alpha}{(v_2^\alpha)^2}$$

Resolution

Underlying microstructure



Every cell Ω_α with boundary $\partial\Omega_\alpha$ can be reconstructed from common curves $\mathcal{I}_{\alpha\gamma}$. Can we solve for $\mathcal{I}_{\alpha\gamma}$?

EGS – Transformation

Solving for parameterizations of common curves $\mathcal{I}_{\alpha\gamma}$ is difficult. To circumvent this difficulty, we introduce a diffeomorphic transformation.

Let every point of a growing ellipse be given by a time-dependent mapping from a unit circle:

$$\varphi_\alpha : S^1 \times (0, \Delta) \rightarrow S_\alpha \subset \mathbb{R}^2$$

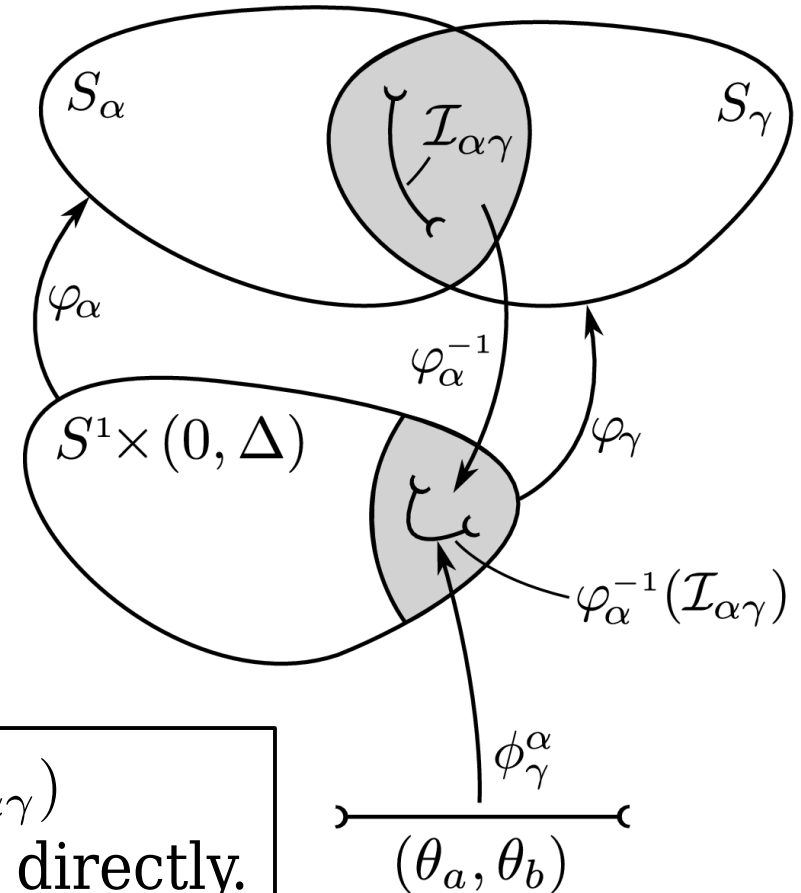
$$: (\underline{x}, t) \mapsto \underline{x}_\alpha + t \mathbf{Z}_\alpha^{-1/2} \cdot \underline{x}$$

We let the common curves be

$$\mathcal{I}_{\alpha\beta} = \{\underline{y} \in S_\alpha \cap S_\beta \mid f_\beta^\alpha(\underline{y}) = 0\}$$

with $f_\beta^\alpha(\underline{y}) = \tau \circ \varphi_\alpha^{-1}(\underline{y}) - \tau \circ \varphi_\beta^{-1}(\underline{y})$.

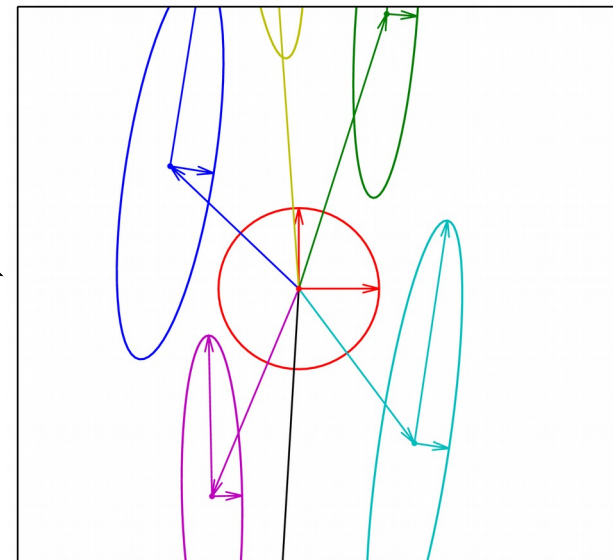
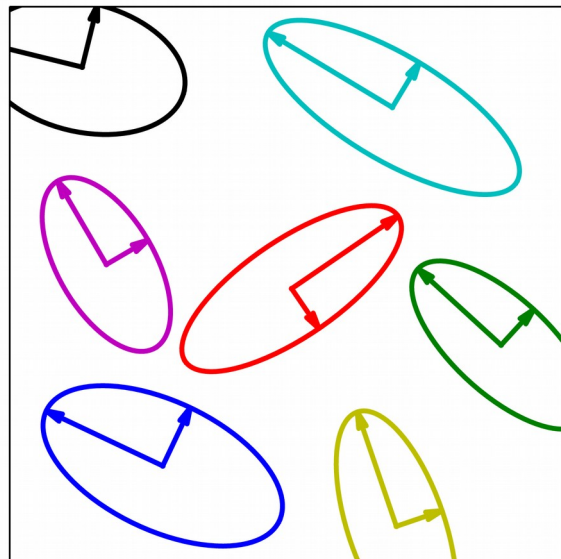
Finding parameterizations ϕ_γ^α of $\varphi_\alpha^{-1}(\mathcal{I}_{\alpha\gamma})$ is much easier than parameterizing $\mathcal{I}_{\alpha\gamma}$ directly.



EGS – Transformation (illustration)

Solving for charts ϕ_γ^α is equivalent to solve for times at which a given point in S^1 is intersected by a moving ellipse of fixed dimensions.

$$\begin{aligned}\phi_\gamma^\alpha : (\theta_a, \theta_b) &\rightarrow S^1 \times (0, \Delta) \\ &: \theta \mapsto (\underline{x}(\theta), \xi_\gamma^\alpha \circ \underline{x}(\theta))\end{aligned}$$



Contact function:

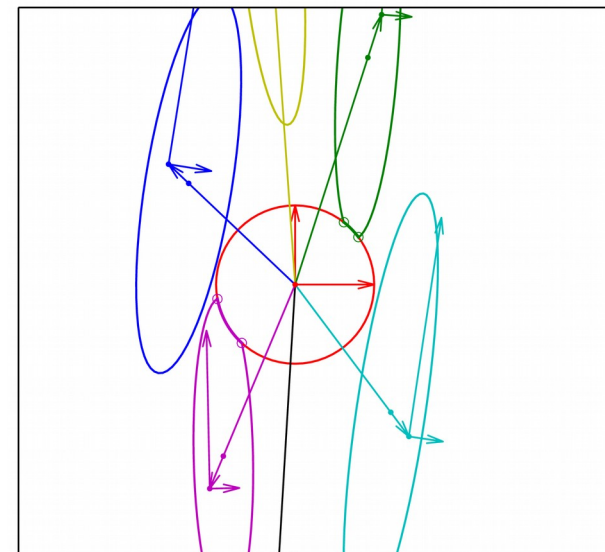
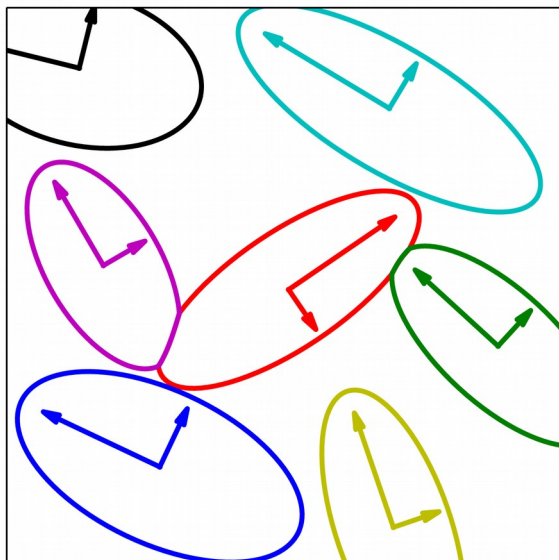
$$\xi_\gamma^\alpha = \frac{\underline{x}_\gamma^\alpha \cdot \mathbf{Z}_\gamma^\alpha \cdot \underline{x}_\gamma^\alpha}{\underline{x}(\theta) \cdot \mathbf{Z}_\gamma^\alpha \cdot \underline{x}_\gamma^\alpha + \delta \sqrt{(\underline{x}(\theta) \cdot \mathbf{Z}_\gamma^\alpha \cdot \underline{x}_\gamma^\alpha)^2 - (\underline{x}_\gamma^\alpha \cdot \mathbf{Z}_\gamma^\alpha \cdot \underline{x}_\gamma^\alpha) [\underline{x}(\theta) \cdot \mathbf{Z}_\gamma^\alpha \cdot \underline{x}(\theta) - 1]}}$$

Still, common points (locations of triple junctions) must be solved numerically.

EGS – Transformation (illustration)

Solving for charts ϕ_γ^α is equivalent to solve for times at which a given point in S^1 is intersected by a moving ellipse of fixed dimensions.

$$\begin{aligned}\phi_\gamma^\alpha : (\theta_a, \theta_b) &\rightarrow S^1 \times (0, \Delta) \\ &: \theta \mapsto (\underline{x}(\theta), \xi_\gamma^\alpha \circ \underline{x}(\theta))\end{aligned}$$



Contact function:

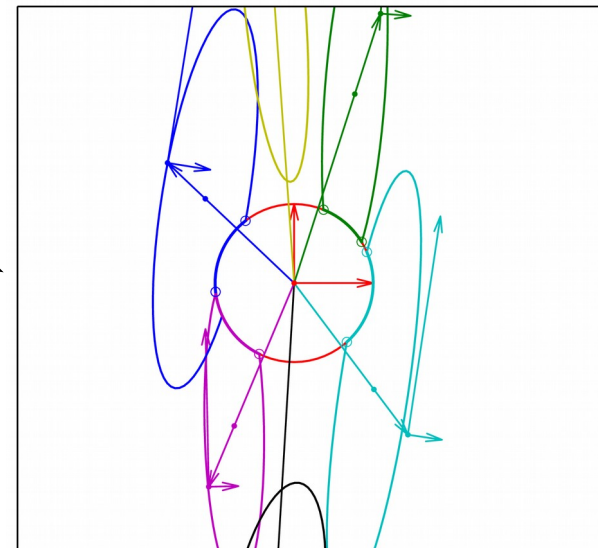
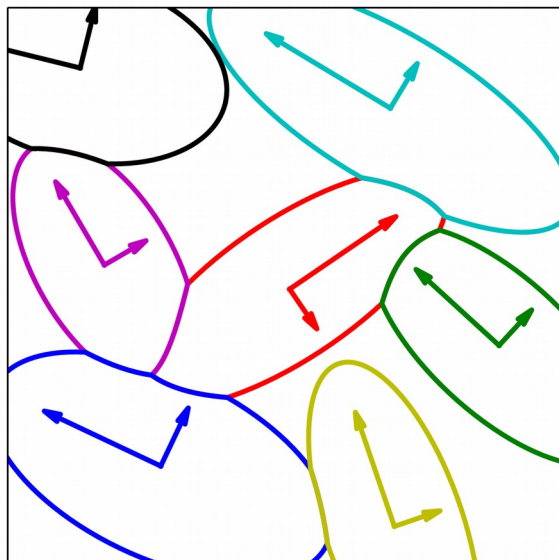
$$\xi_\gamma^\alpha = \frac{\underline{x}_\gamma^\alpha \cdot \mathbf{Z}_\gamma^\alpha \cdot \underline{x}_\gamma^\alpha}{\underline{x}(\theta) \cdot \mathbf{Z}_\gamma^\alpha \cdot \underline{x}_\gamma^\alpha + \delta \sqrt{(\underline{x}(\theta) \cdot \mathbf{Z}_\gamma^\alpha \cdot \underline{x}_\gamma^\alpha)^2 - (\underline{x}_\gamma^\alpha \cdot \mathbf{Z}_\gamma^\alpha \cdot \underline{x}_\gamma^\alpha) [\underline{x}(\theta) \cdot \mathbf{Z}_\gamma^\alpha \cdot \underline{x}(\theta) - 1]}}$$

Still, common points (locations of triple junctions) must be solved numerically.

EGS – Transformation (illustration)

Solving for charts ϕ_γ^α is equivalent to solve for times at which a given point in S^1 is intersected by a moving ellipse of fixed dimensions.

$$\begin{aligned}\phi_\gamma^\alpha : (\theta_a, \theta_b) &\rightarrow S^1 \times (0, \Delta) \\ : \theta &\mapsto (\underline{x}(\theta), \xi_\gamma^\alpha \circ \underline{x}(\theta))\end{aligned}$$



Contact function:

$$\xi_\gamma^\alpha = \frac{\underline{x}_\gamma^\alpha \cdot \mathbf{Z}_\gamma^\alpha \cdot \underline{x}_\gamma^\alpha}{\underline{x}(\theta) \cdot \mathbf{Z}_\gamma^\alpha \cdot \underline{x}_\gamma^\alpha + \delta \sqrt{(\underline{x}(\theta) \cdot \mathbf{Z}_\gamma^\alpha \cdot \underline{x}_\gamma^\alpha)^2 - (\underline{x}_\gamma^\alpha \cdot \mathbf{Z}_\gamma^\alpha \cdot \underline{x}_\gamma^\alpha) [\underline{x}(\theta) \cdot \mathbf{Z}_\gamma^\alpha \cdot \underline{x}(\theta) - 1]}}$$

Still, common points (locations of triple junctions) must be solved numerically.

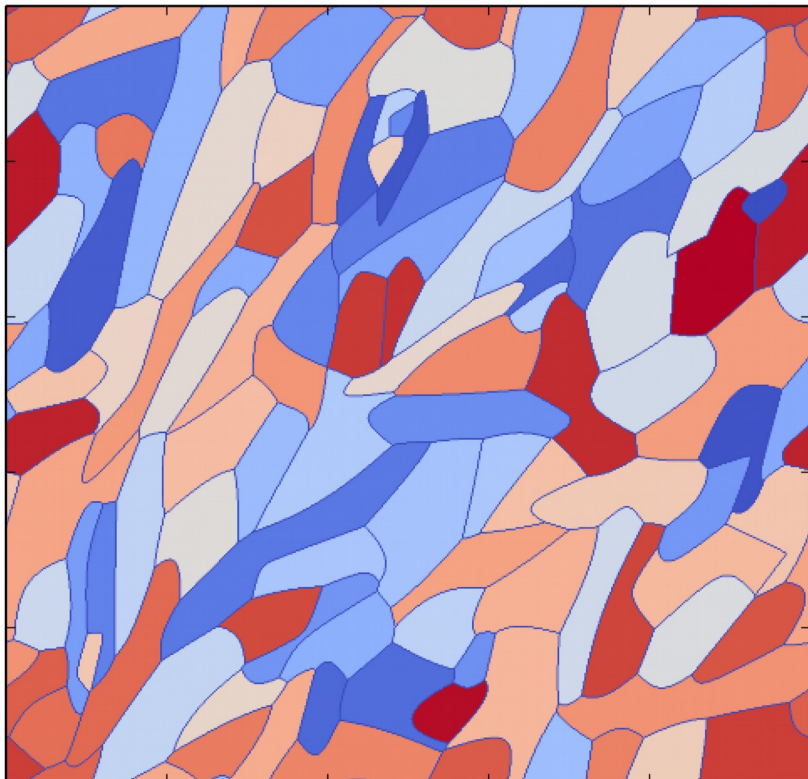
Ellipsoidal growth structures as microstructure models

For the same definition of common curves, i.e. f_γ^α , we try to generate different types of underlying microstructures by changing the contact functions.

Space filling models (Tess.):

$$\xi_\gamma^\alpha = \tilde{\xi}_\gamma^\alpha$$

(1 common curve per pair of neighbors)



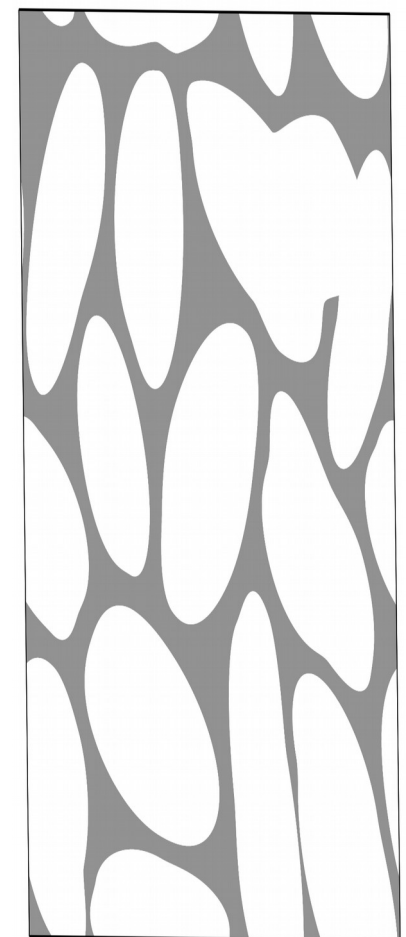
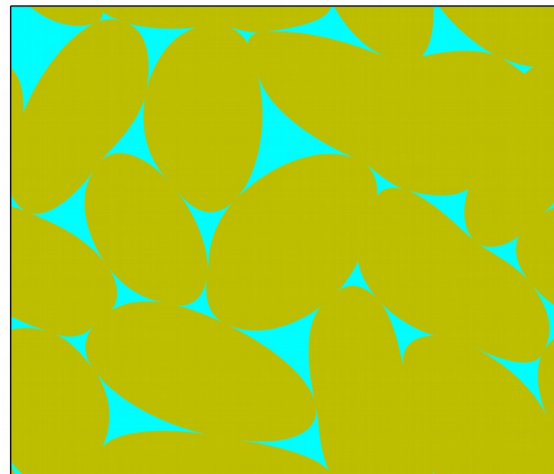
Non-space filling models:

$$\xi_\gamma^\alpha \leq \tilde{\xi}_\gamma^\alpha$$



$$\mathcal{I}_{\alpha\gamma} \neq \mathcal{I}_{\gamma\alpha}$$

(2 common curves per pair of neighbors)



Space filling EGS – Parameterization (Define d_γ^α)

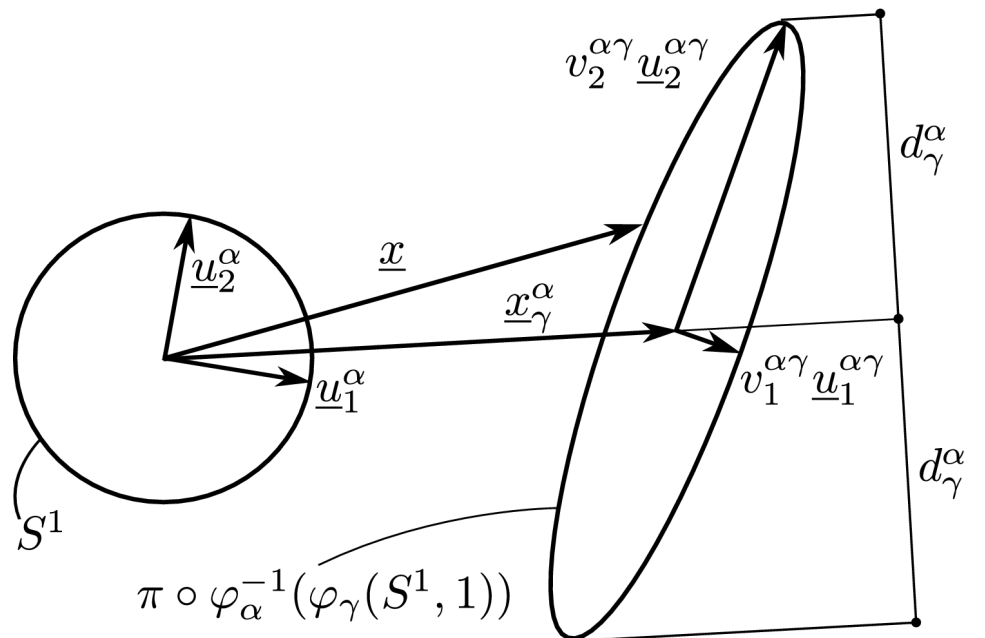
To solve for a parameterization of the common curve $\tilde{\mathcal{I}}_{\alpha\gamma} \subset \mathcal{I}_{\alpha\gamma}$, we first define the distance d_γ^α :

Convention for the spectral decomposition of \mathbf{Z}_γ^α :

$$\underline{u}_1^{\alpha\gamma} \cdot \underline{x}_\gamma^\alpha \geq 0$$

$$v_2^{\alpha\gamma} \geq v_1^{\alpha\gamma} > 0$$

$$\underline{u}_1^{\alpha\gamma} \times \underline{u}_2^{\alpha\gamma} = \underline{u}_1^\alpha \times \underline{u}_2^\alpha$$



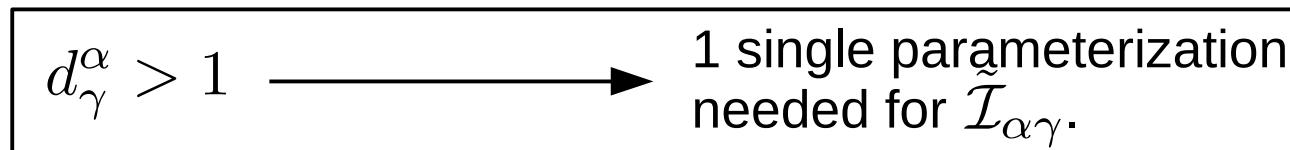
This distance is given by $d_\gamma^\alpha \equiv \max_{x \in \pi \circ \varphi_\alpha^{-1}(\varphi_\gamma(S^1, 1))} \|\underline{x}_\alpha\|^{-1} \underline{x} \cdot \mathbf{R}_{\pi/2} \cdot \underline{x}_\gamma^\alpha$

where $\mathbf{R}_\theta = \underline{u}_k^{\alpha\gamma} \otimes \underline{u}_k^{\alpha\gamma} \cos \theta + \epsilon_{j i 3} \underline{u}_i^{\alpha\gamma} \otimes \underline{u}_j^{\alpha\gamma} \sin \theta$ so that $\mathbf{R}_\theta \cdot \underline{x}$ is an active counterclockwise θ rad rotation of \underline{x} .

We find
$$d_\gamma^\alpha = \|\underline{x}_\gamma^\alpha\|^{-1} \sqrt{(v_2^{\alpha\gamma} \underline{u}_1^{\alpha\gamma} \cdot \underline{x}_\gamma^\alpha)^2 + (v_1^{\alpha\gamma} \underline{u}_2^{\alpha\gamma} \cdot \underline{x}_\gamma^\alpha)^2}.$$

Space filling EGS – Parameterization (Cases w/ $d_\gamma^\alpha > 1$)

The parameterization of the common curve $\tilde{\mathcal{I}}_{\alpha\gamma}$ strongly depends on the distance d_γ^α . First, we consider:



Let ${}^k\phi_\gamma^\alpha : ({}^k\theta_a, {}^k\theta_b) \rightarrow V \subset S^1 \times (0, \Delta)$

$$: \theta \mapsto (\underline{x}(\theta), {}^k\xi_\gamma^\alpha \circ \underline{x}(\theta)) \quad | \quad {}^k\xi_\gamma^\alpha(\pi \circ \varphi_\alpha^{-1}({}^k\tilde{\mathcal{I}}_{\alpha\gamma})) = \tau \circ \varphi_\alpha^{-1}({}^k\tilde{\mathcal{I}}_{\alpha\gamma})$$

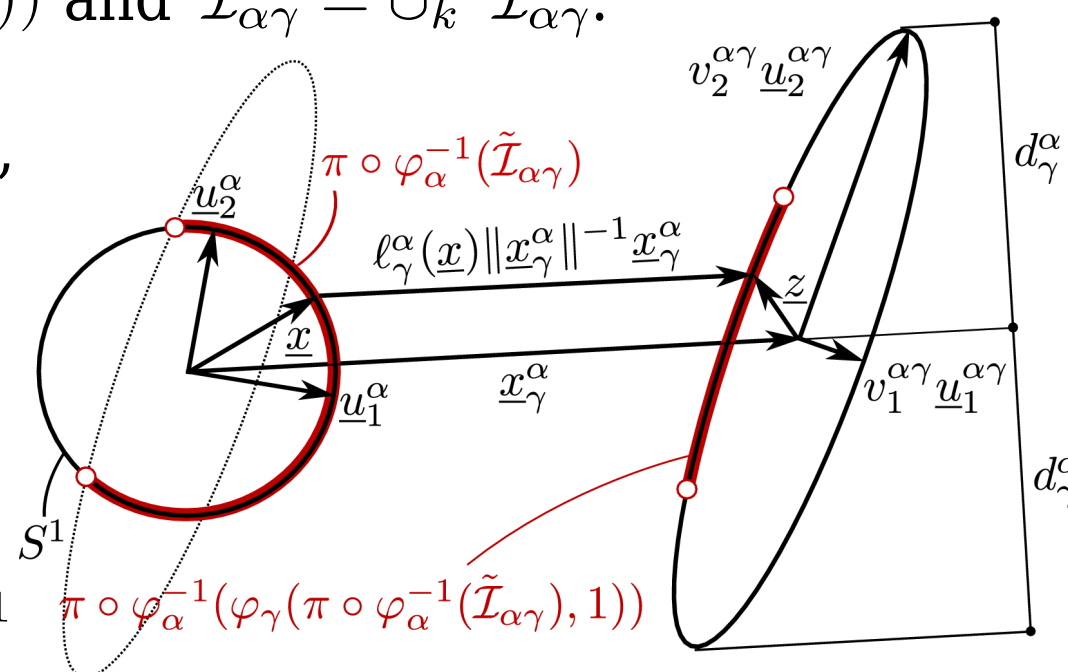
such that ${}^k\tilde{\mathcal{I}}_{\alpha\gamma} = \varphi_\alpha({}^k\phi_\gamma^\alpha(({}^k\theta_a, {}^k\theta_b)))$ and $\tilde{\mathcal{I}}_{\alpha\gamma} = \cup_k {}^k\tilde{\mathcal{I}}_{\alpha\gamma}$.

Let $\underline{z} = \underline{u}_1^{\alpha\gamma} v_1^{\alpha\gamma} \cos \theta + \underline{u}_2^{\alpha\gamma} v_2^{\alpha\gamma} \sin \theta$,

and solve for $\ell_\gamma^\alpha(\underline{x})$ such that

$$\underline{x}_\gamma^\alpha + \underline{z} - \ell_\gamma^\alpha(\underline{x}) \|\underline{x}_\gamma^\alpha\|^{-1} \underline{x}_\gamma^\alpha \in S^1.$$

From the def. of φ_α , we find
that ${}^k\xi_\gamma^\alpha(\underline{x}) = \|\underline{x}_\gamma^\alpha\| (\|\underline{x}_\gamma^\alpha\| - \ell_\gamma^\alpha(\underline{x}))^{-1}$



ADD DETAILS.

Space filling EGS – Parameterization (Cases w/ $d_\gamma^\alpha > 1$)

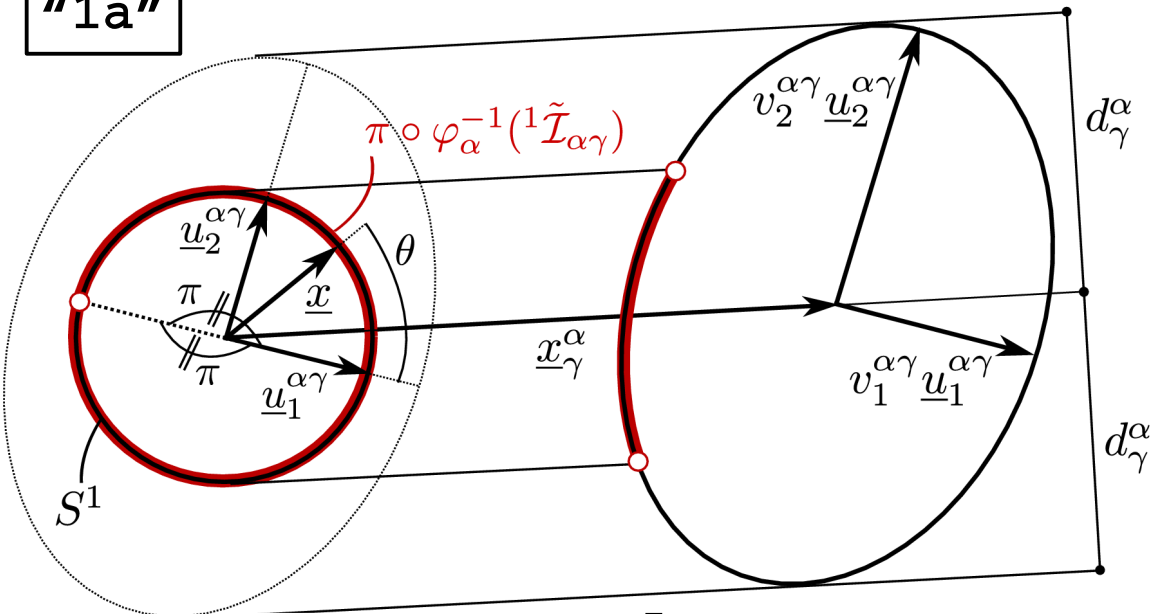
As a result, we find

$${}^k \xi_\gamma^\alpha = \frac{\underline{x}_\gamma^\alpha \cdot \mathbf{Z}_\gamma^\alpha \cdot \underline{x}_\gamma^\alpha}{\underline{x} \cdot \mathbf{Z}_\gamma^\alpha \cdot \underline{x}_\gamma^\alpha + {}^k \delta \sqrt{(\underline{x} \cdot \mathbf{Z}_\gamma^\alpha \cdot \underline{x}_\gamma^\alpha)^2 - (\underline{x}_\gamma^\alpha \cdot \mathbf{Z}_\gamma^\alpha \cdot \underline{x}_\gamma^\alpha) [x \cdot \mathbf{Z}_\gamma^\alpha \cdot x - 1]}}$$

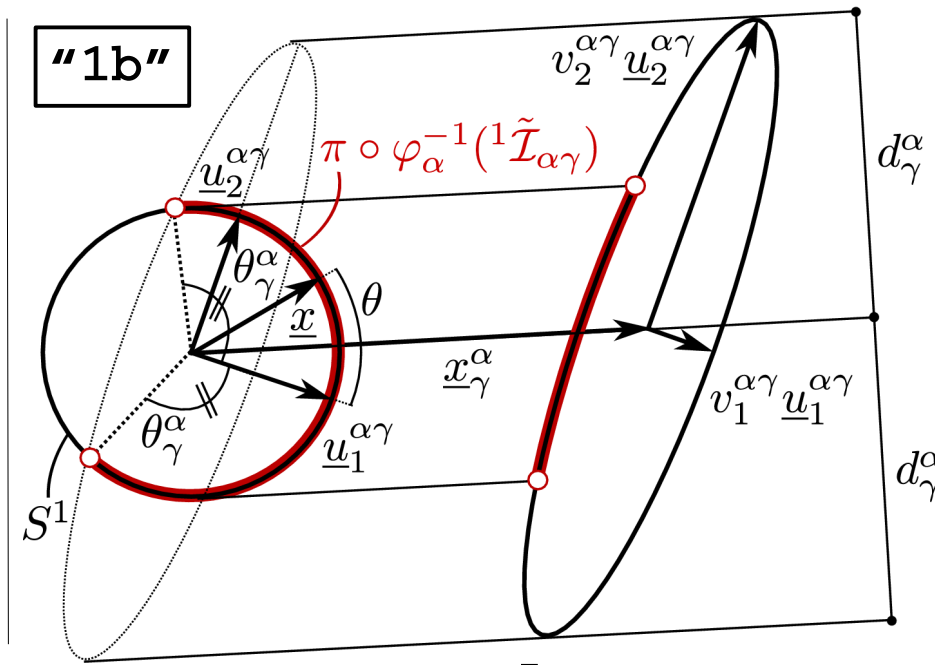
where ${}^k \delta = \pm 1$ and $\underline{x} \in {}^k \phi_\gamma^\alpha(({}^k \theta_a, {}^k \theta_b)) \subset S^1$. For $d_\gamma^\alpha > 1$, we have $\tilde{\mathcal{I}}_{\alpha\gamma} = {}^1 \tilde{\mathcal{I}}_{\alpha\gamma}$ and ${}^1 \delta = 1$. As we let $\underline{x} : \theta \mapsto \underline{u}_1^{\alpha\gamma} \cos \theta + \underline{u}_2^{\alpha\gamma} \sin \theta$, we obtain:

$$({}^1 \theta_a, {}^1 \theta_b) = (-\pi, \pi) \text{ if } v_1^{\alpha\gamma} \geq v_2^{\alpha\gamma} \geq 1 , \quad ({}^1 \theta_a, {}^1 \theta_b) = (-\theta_\alpha^\gamma, \theta_\alpha^\gamma) \text{ otherwise.}$$

"1a"



"1b"



$$\text{where } \theta_\alpha^\gamma = \pi - \text{atan} \left[(v_2^{\alpha\gamma}/v_1^{\alpha\gamma}) \sqrt{[(v_1^{\alpha\gamma})^2 - 1]/[1 - (v_2^{\alpha\gamma})^2]} \right].$$

Space filling EGS – Parameterization (Cases w/ $d_\gamma^\alpha \leq 1$)

Otherwise, we have:

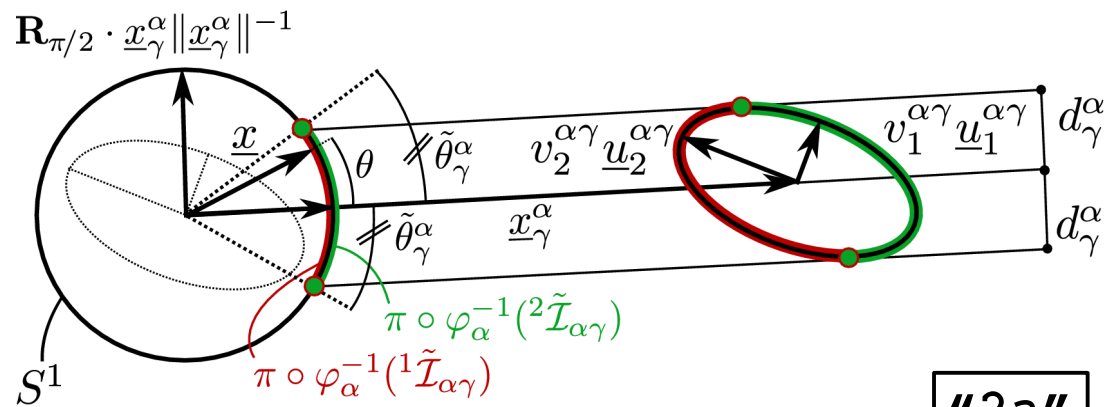
$$d_\gamma^\alpha \leq 1$$

More than 1 parameterization
needed for $\tilde{\mathcal{I}}_{\alpha\gamma}$.

Then, the common curve is parameterized with $\underline{x} : \theta \mapsto \|\underline{x}_\gamma^\alpha\|^{-1} \mathbf{R}_\theta \cdot \underline{x}_\gamma^\alpha$ and ${}^k \xi_\gamma^\alpha$ is defined as previously so that $\tilde{\mathcal{I}}_{\alpha\gamma} = \cup_k {}^k \tilde{\mathcal{I}}_{\alpha\gamma}$ where $k = 2$ or 3 , ${}^1 \delta = 1$ and ${}^2 \delta = {}^3 \delta = -1$.

First, a special case is defined as follows, if $v_1^{\alpha\gamma} \leq v_2^{\alpha\gamma} \leq 1$:

$$\begin{aligned}\tilde{\mathcal{I}}_{\alpha\gamma} &= \cup_{k=1}^2 {}^k \tilde{\mathcal{I}}_{\alpha\gamma} \\ ({}^1 \theta_a, {}^1 \theta_b) &= (-\tilde{\theta}_\gamma^\alpha, \tilde{\theta}_\gamma^\alpha) \\ ({}^2 \theta_a, {}^2 \theta_b) &= (-\tilde{\theta}_\gamma^\alpha, \tilde{\theta}_\gamma^\alpha)\end{aligned}$$



"2a"

where $\tilde{\theta}_\gamma^\alpha = \arcsin(d_\gamma^\alpha)$.

Space filling EGS – Parameterization (Cases w/ $d_\gamma^\alpha \leq 1$)

- if $\text{not}(v_1^{\alpha\gamma} \leq v_2^{\alpha\gamma} \leq 1)$ and $\underline{u}_2^{\alpha\gamma} \cdot \underline{x}_\gamma^\alpha > 0$:

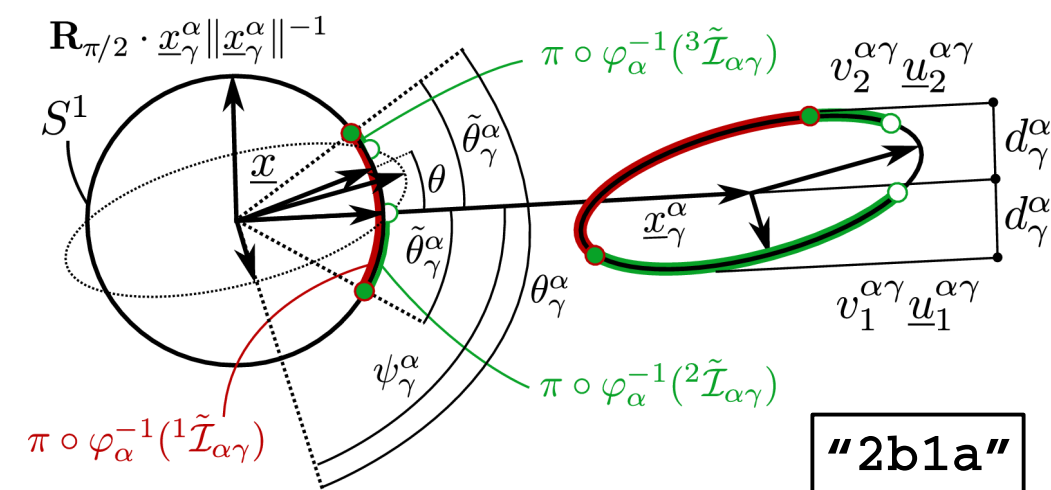
- if ${}^1\xi_\gamma^\alpha(\tilde{\theta}_\gamma^\alpha) > 0$:

$$\tilde{\mathcal{I}}_{\alpha\gamma} = \cup_{k=1}^3 {}^k\tilde{\mathcal{I}}_{\alpha\gamma}$$

$$({}^1\theta_a, {}^1\theta_b) = (-\tilde{\theta}_\gamma^\alpha, \tilde{\theta}_\gamma^\alpha)$$

$$({}^2\theta_a, {}^2\theta_b) = (-\tilde{\theta}_\gamma^\alpha, \pi - \theta_\gamma^\alpha - \psi_\gamma^\alpha)$$

$$({}^3\theta_a, {}^3\theta_b) = (\theta_\gamma^\alpha - \psi_\gamma^\alpha, \tilde{\theta}_\gamma^\alpha)$$

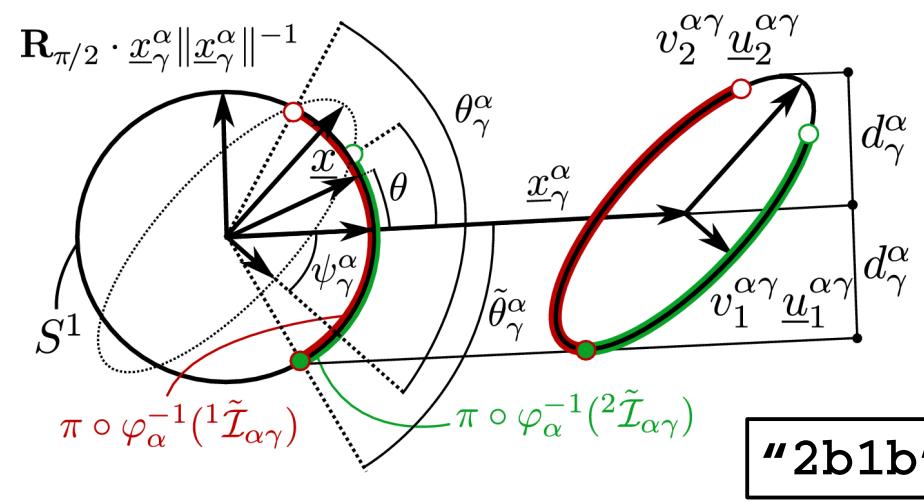


- otherwise :

$$\tilde{\mathcal{I}}_{\alpha\gamma} = \cup_{k=1}^2 {}^k\tilde{\mathcal{I}}_{\alpha\gamma}$$

$$({}^1\theta_a, {}^1\theta_b) = (-\tilde{\theta}_\gamma^\alpha, \theta_\gamma^\alpha - \psi_\gamma^\alpha)$$

$$({}^2\theta_a, {}^2\theta_b) = (-\tilde{\theta}_\gamma^\alpha, \pi - \theta_\gamma^\alpha - \psi_\gamma^\alpha)$$



- where $\tilde{\theta}_\gamma^\alpha = \arcsin(d_\gamma^\alpha)$ and $\psi_\gamma^\alpha = \arccos(\underline{u}_1^{\alpha\gamma} \cdot \underline{x}_\gamma^\alpha ||\underline{x}_\gamma^\alpha||^{-1})$.

Space filling EGS – Parameterization (Cases w/ $d_\gamma^\alpha \leq 1$)

- if $\text{not}(v_1^{\alpha\gamma} \leq v_2^{\alpha\gamma} \leq 1)$ and $\underline{u}_2^{\alpha\gamma} \cdot \underline{x}_\gamma^\alpha \leq 0$:

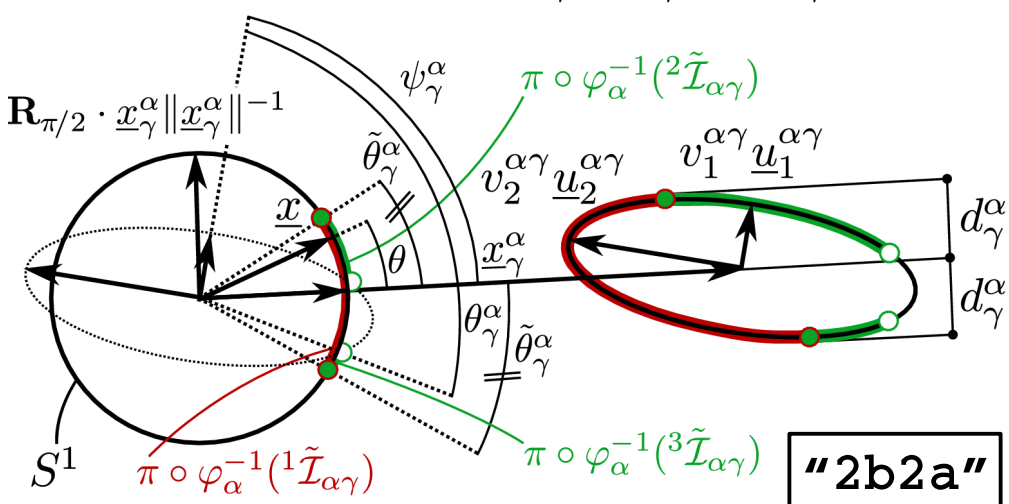
- if ${}^1\xi_\gamma^\alpha(-\tilde{\theta}_\gamma^\alpha) > 0$:

$$\tilde{\mathcal{I}}_{\alpha\gamma} = \cup_{k=1}^3 {}^k\tilde{\mathcal{I}}_{\alpha\gamma}$$

$$({}^1\theta_a, {}^1\theta_b) = (-\tilde{\theta}_\gamma^\alpha, \tilde{\theta}_\gamma^\alpha)$$

$$({}^2\theta_a, {}^2\theta_b) = (\theta_\gamma^\alpha + \psi_\gamma^\alpha - \pi, \tilde{\theta}_\gamma^\alpha)$$

$$({}^3\theta_a, {}^3\theta_b) = (-\tilde{\theta}_\gamma^\alpha, \psi_\gamma^\alpha - \theta_\gamma^\alpha)$$

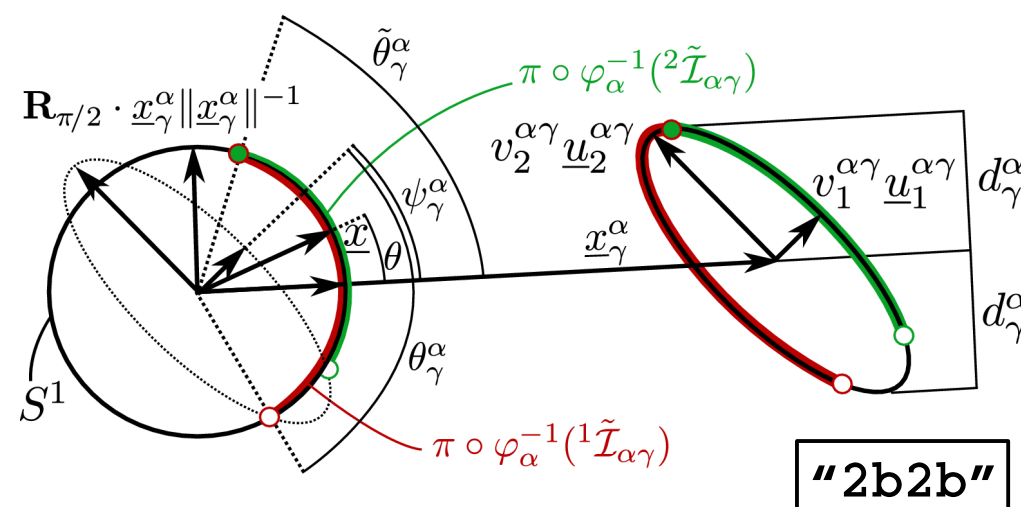


- otherwise :

$$\tilde{\mathcal{I}}_{\alpha\gamma} = \cup_{k=1}^2 {}^k\tilde{\mathcal{I}}_{\alpha\gamma}$$

$$({}^1\theta_a, {}^1\theta_b) = (\psi_\gamma^\alpha - \theta_\gamma^\alpha, \tilde{\theta}_\gamma^\alpha)$$

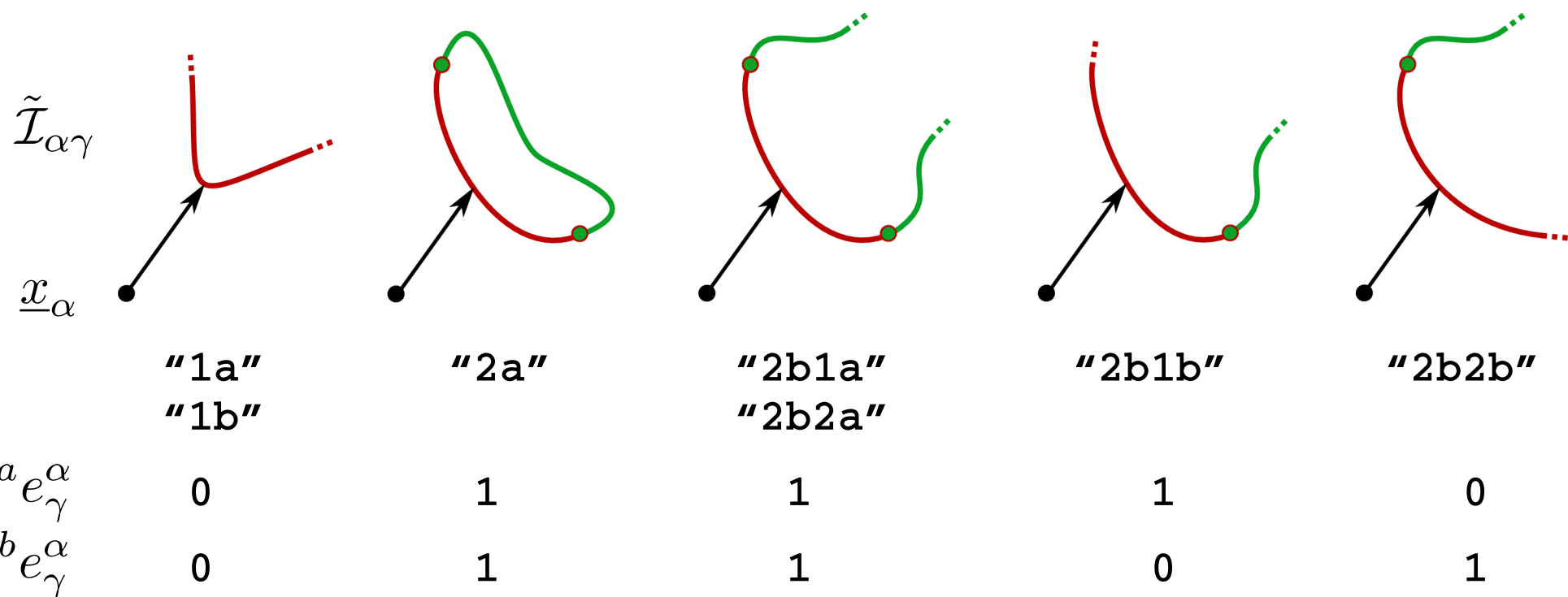
$$({}^2\theta_a, {}^2\theta_b) = (\theta_\gamma^\alpha + \psi_\gamma^\alpha - \pi, \tilde{\theta}_\gamma^\alpha)$$



- where $\tilde{\theta}_\gamma^\alpha = \arcsin(d_\gamma^\alpha)$ and $\psi_\gamma^\alpha = \arccos(\underline{u}_1^{\alpha\gamma} \cdot \underline{x}_\gamma^\alpha \|\underline{x}_\gamma^\alpha\|^{-1})$.

Space filling EGS – Solve for Common Points

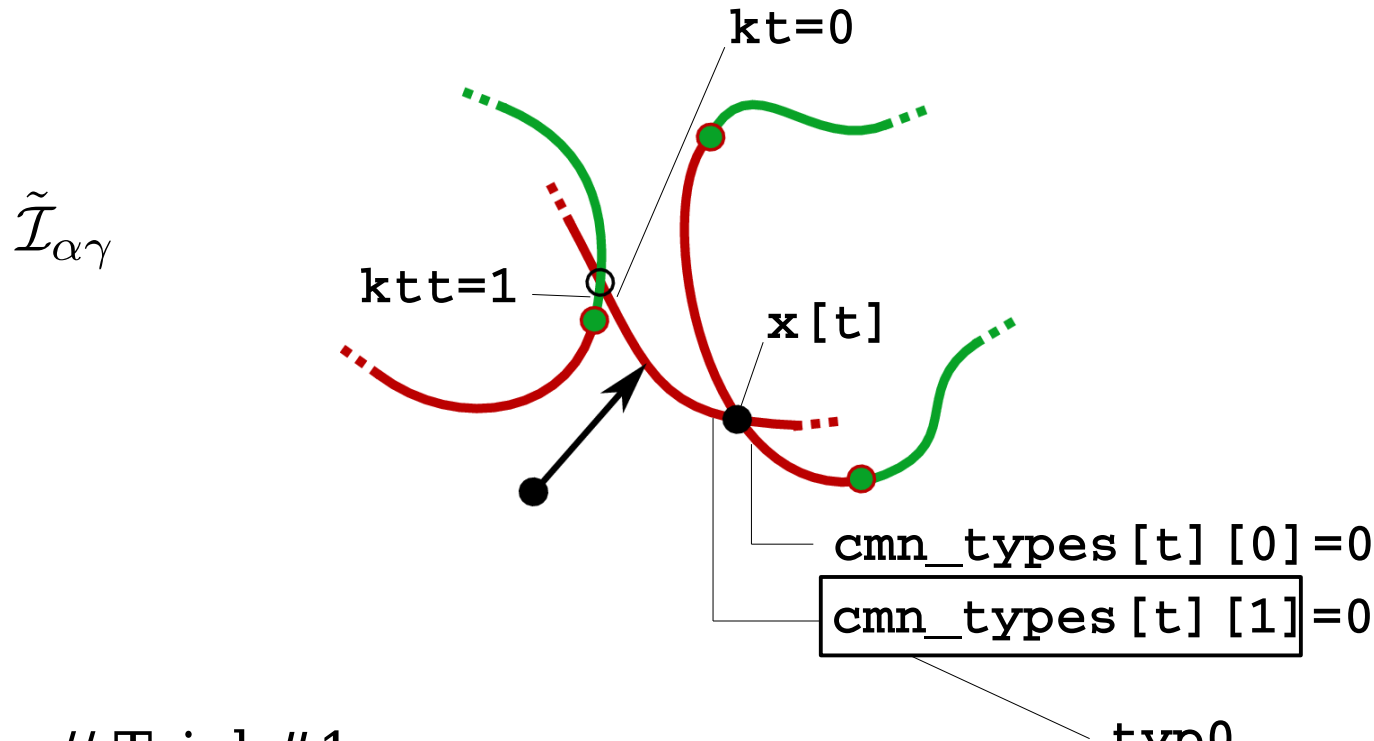
We summarize and classify the different types of parameterized common curves as follows:



where ${}^a e_\gamma^\alpha$ and ${}^b e_\gamma^\alpha$ are defined to solve for common points.

Space filling EGS – Solve for Common Points

Given a common point $\mathbf{x}[t]$ found at the intersection of two common curves, we want to find the next common point of the cell boundary:



```
kt=0,ktt=0 // Trial #1
kt=1,ktt=0 // Trial #2
kt=0,ktt=1 // Trial #3
```

Expressions of Minkowski tensors for EGS

Using the parameterization of the EGS, the following expressions are obtained:

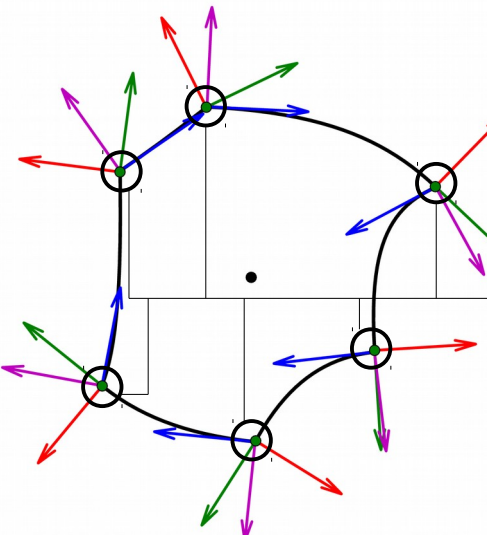
$$\mathcal{W}_0^{r,0} = \sum_{i=0}^r \sum_{j=0}^{r-i} \binom{r}{i+j} \underline{x}_\alpha^{\otimes r-i-j} \odot \underline{u}_1^{\alpha \otimes i} \odot \underline{u}_2^{\alpha \otimes j} I_0^{i,j}$$

\underline{x}_α , \underline{u}_1^α and \underline{u}_2^α are from the MPP.

$$\mathcal{W}_1^{r,s} = \sum_{i=0}^r \sum_{j=0}^{r-i} \sum_{k=0}^s \binom{r}{i+j} \binom{s}{k} \underline{x}_\alpha^{\otimes r-i-j} \odot \underline{u}_1^{\alpha \otimes s+i-k} \odot \underline{u}_2^{\alpha \otimes j+k} I_1^{i,j,k,s-k}$$

$$\mathcal{W}_2^{r,s} = \sum_{i=0}^r \sum_{j=0}^{r-i} \sum_{k=0}^s \binom{r}{i+j} \binom{s}{k} \underline{x}_\alpha^{\otimes r-i-j} \odot \underline{u}_1^{\alpha \otimes s+i-k} \odot \underline{u}_2^{\alpha \otimes j+k} I_2^{i,j,k,s-k} + \sum_{\underline{y} \in \mathcal{K}_\alpha} \mathcal{D}^{r,s}(\underline{y})$$

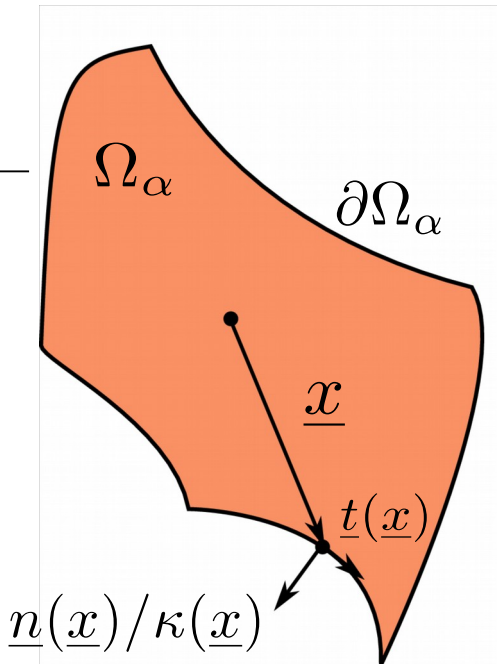
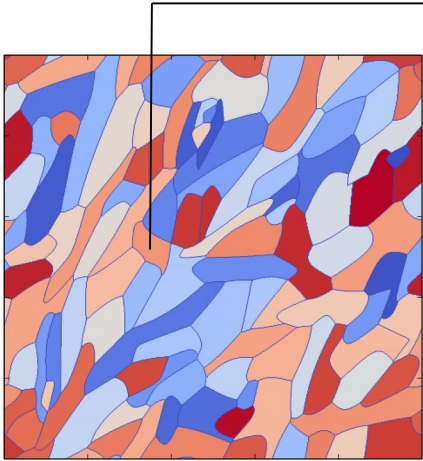
where $I_0^{i,j}$ and $I_\nu^{i,j,k,l}$ are scalar coefficients obtained by integration of the locally defined contact functions ξ .



Effect of common points

Morphological characterization

Single grains are characterized using Minkowski tensors:



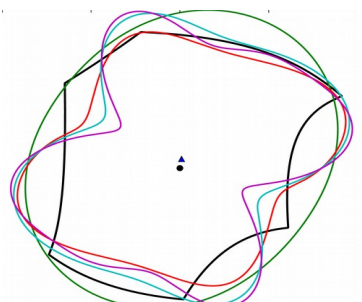
Reynolds glyphs of Minkowski tensors

— : $r + s = 2$

— : $r + s = 4$

— : $r + s = 6$

— : $r + s = 8$



$\mathcal{W}_1^{0,s}$

$\mathcal{W}_1^{r,0}$

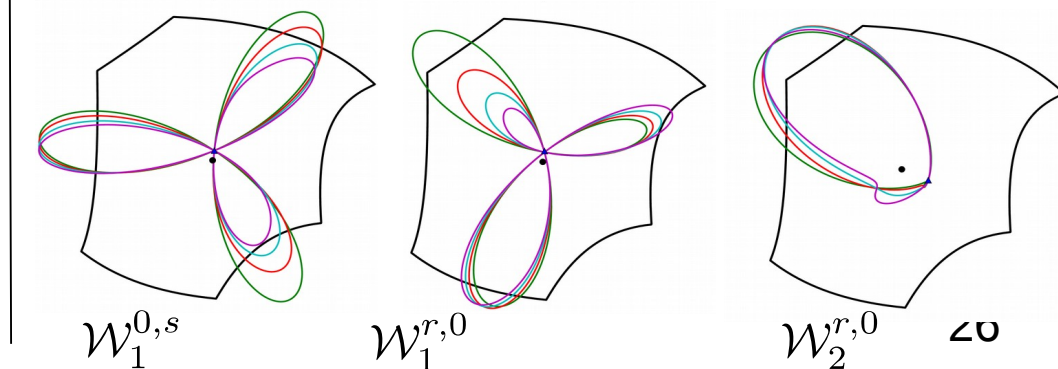
$\mathcal{W}_2^{r,0}$

— : $r + s = 3$

— : $r + s = 5$

— : $r + s = 7$

— : $r + s = 9$



$\mathcal{W}_1^{0,s}$

$\mathcal{W}_1^{r,0}$

$\mathcal{W}_2^{r,0}$

ω

Measures of mass distribution:

$$\mathcal{W}_0^{r,0} = \int_{\Omega_\alpha} \underline{x}^{\otimes r} dV$$

Measures of surface distribution:

$$\mathcal{W}_1^{r,s} = \int_{\partial\Omega_\alpha} \underline{x}^{\otimes r} \odot [\underline{n}(x)]^{\otimes s} dS$$

Curvature-weighted measures of surface distribution:

$$\mathcal{W}_2^{r,s} = \int_{\partial\Omega_\alpha} \kappa(x) \underline{x}^{\otimes r} \odot [\underline{n}(x)]^{\otimes s} dS$$

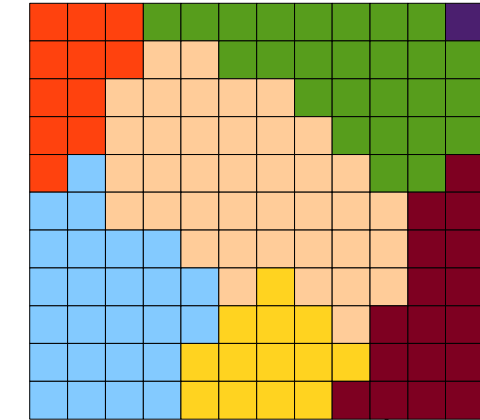
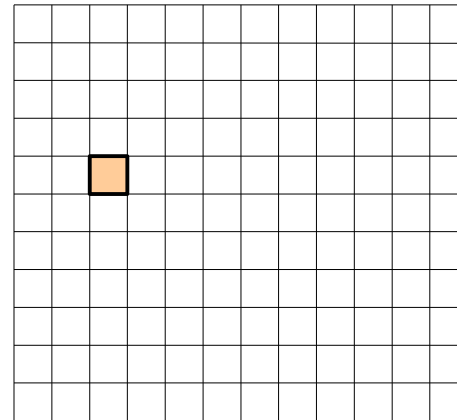
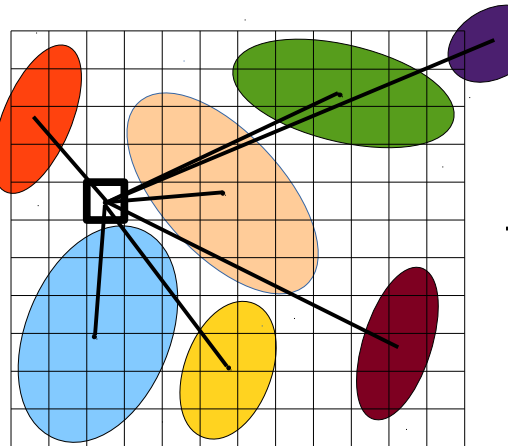
EGS – Resolution

I) Discretize and solve numerically for lists of neighbors.

Compute contact times,

attribute pixel,

and repeat for each pixel.



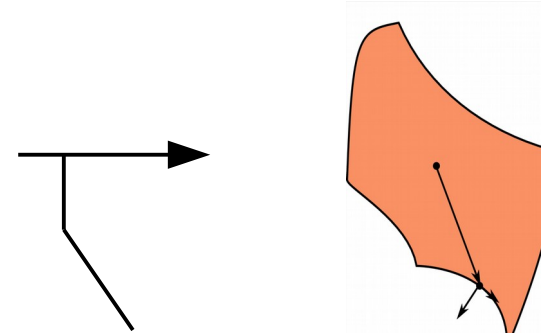
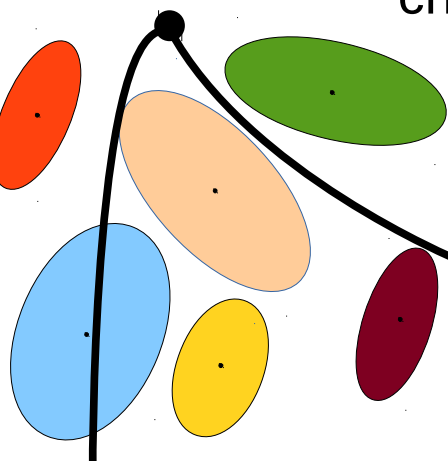
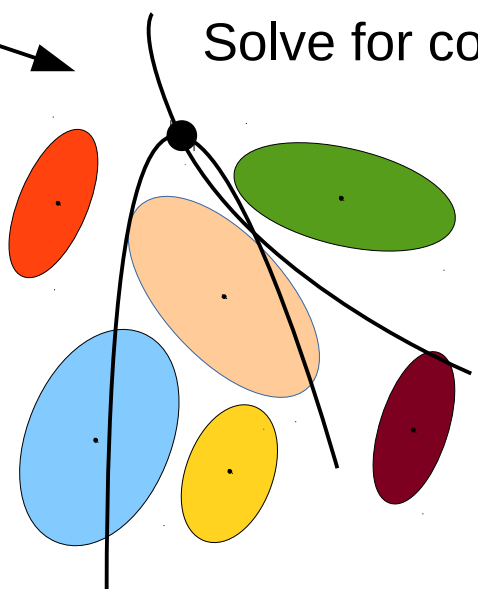
Get list of neighbors

II) Solve for common points with parameterizations of common curves.

Solve for common point,

select & bound local charts,

and repeat for each neighbor.

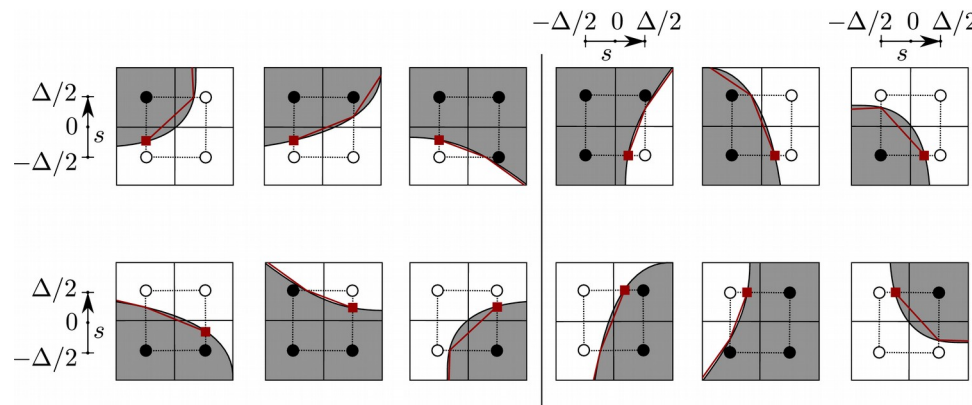


Get atlas of cell boundary.

Enriched Marching Squares (EMS)

Objective: Approximate Minkowski tensors with higher accuracy from coarse resolution of tessellations

Method: Use our parametric representation of grain boundaries to derive a more efficient Marching square algorithm:

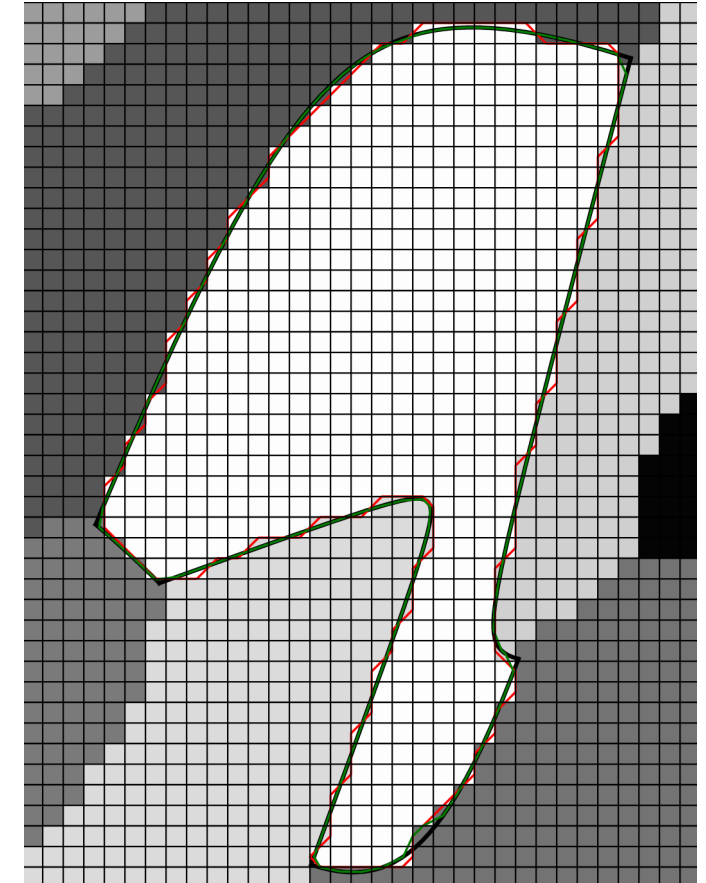


Minkowski tensors of n -polytopes

$$\mathcal{W}_0^{r,0}(\mathcal{C}) = \frac{1}{r+2} \sum_{k=1}^n \sum_{i=0}^{r+1} \sum_{j=0}^i \binom{r+1}{i} \binom{i}{j} \frac{(-1)^{i-j} L_k}{i+1} \left[\underline{v}_k^{\otimes r+1-j} \odot \underline{v}_{k+1}^{\otimes j} \right] \cdot \underline{n}_k, \quad (1)$$

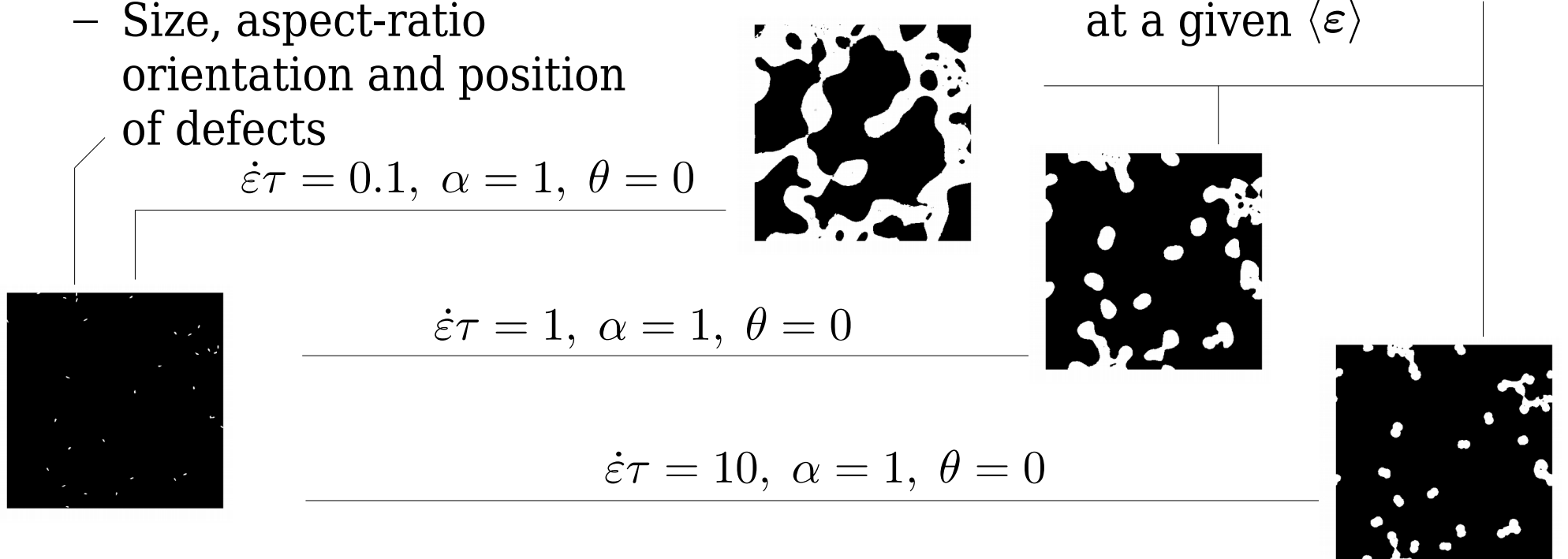
$$\mathcal{W}_1^{r,s}(\mathcal{C}) = \frac{1}{2} \sum_{k=1}^n \sum_{i=0}^r \sum_{j=0}^i \binom{r}{i} \binom{i}{j} \frac{(-1)^{i-j} L_k}{i+1} \underline{v}_k^{\otimes r-j} \odot \underline{v}_{k+1}^{\otimes j} \odot \underline{n}_k^{\otimes s}, \quad (2)$$

$$\mathcal{W}_2^{r,s}(\mathcal{C}) = \frac{1}{2} \sum_{k=1}^n \sum_{i=0}^s \sum_{j=0}^i \binom{s}{i} \binom{i}{j} \frac{(-1)^{i-j}}{L_k^i} \underline{v}_k^{\otimes i-j} \odot \underline{v}_{k+1}^{\otimes r+j} \odot \underline{n}_k^{\otimes s-i} I_k^{s,i}(\Delta\theta_k) \quad (3)$$



Application #1 / Viscoplastic matrix with random defects

Quantify the morphological uncertainty of plastic regions

- Constitutive model: $\dot{\sigma}(t) = \mathbb{L} : [\dot{\epsilon}(t) - \dot{\epsilon}^p(t)]$ • ICs: $\sigma(0) = \mathbf{0}, \epsilon^p(0) = \mathbf{0}$
 - $f(t) = \|\mathbf{s}(t)\| - s_0$
 - $\mathbf{s}(t) = \text{dev}_{2D}\boldsymbol{\sigma}(t), \|\dot{\epsilon}^p\|(t) = \frac{1}{\tau} \left[\left(\frac{\|\mathbf{s}(t)\|}{s_0} \right)^{\frac{1}{\epsilon}} - 1 \right]$
 - Loading: Mean constant strain rate, $\langle \epsilon \rangle(t) = t \dot{\epsilon} \mathbf{R}_\theta \cdot (\underline{e}_1 \otimes \underline{e}_1 + \alpha \underline{e}_2 \otimes \underline{e}_2) \cdot \mathbf{R}_\theta^t$
 - Material properties: 2D isotropic stiffness; $\kappa_{2D} = 2\mu_{2D}, \mu_{2D} = 10^2 s_0, \epsilon = .5$
 - Sources of randomness:
 - Size, aspect-ratio orientation and position of defects
 - Quantity of interest: Porous-plastified zone at a given $\langle \epsilon \rangle$
- 

 $\dot{\epsilon}\tau = 0.1, \alpha = 1, \theta = 0$

 $\dot{\epsilon}\tau = 1, \alpha = 1, \theta = 0$

 $\dot{\epsilon}\tau = 10, \alpha = 1, \theta = 0$

Application #1 / Viscoplastic matrix with random defects

Quantify the morphological uncertainty of plastic regions

- Constitutive model: $\dot{\sigma}(t) = \mathbb{L} : [\dot{\epsilon}(t) - \dot{\epsilon}^p(t)]$ • ICs: $\sigma(0) = \mathbf{0}, \epsilon^p(0) = \mathbf{0}$
 - $f(t) = \|\mathbf{s}(t)\| - s_0$
 - $\mathbf{s}(t) = \text{dev}_{2D}\boldsymbol{\sigma}(t), \|\dot{\epsilon}^p\|(t) = \frac{1}{\tau} \left[\left(\frac{\|\mathbf{s}(t)\|}{s_0} \right)^{\frac{1}{\epsilon}} - 1 \right]$
 - Loading: Mean constant strain rate, $\langle \epsilon \rangle(t) = t \dot{\epsilon} \mathbf{R}_\theta \cdot (\underline{e}_1 \otimes \underline{e}_1 + \alpha \underline{e}_2 \otimes \underline{e}_2) \cdot \mathbf{R}_\theta^t$
 - Material properties: 2D isotropic stiffness; $\kappa_{2D} = 2\mu_{2D}, \mu_{2D} = 10^2 s_0, \epsilon = .5$
 - Sources of randomness:
 - Size, aspect-ratio orientation and position of defects
 - Quantity of interest: Porous-plastified zone at a given $\langle \epsilon \rangle$
-
- | | |
|--|--|
| $\dot{\epsilon}\tau = 0.1, \alpha = 1, \theta = 0$ | |
| $\dot{\epsilon}\tau = 1, \alpha = 1, \theta = 0$ | |
| $\dot{\epsilon}\tau = 10, \alpha = 1, \theta = 0$ | |

Application #1 / Viscoplastic matrix with random defects

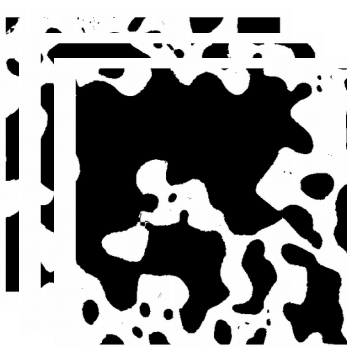
Quantify the morphological uncertainty of plastic regions

- Constitutive model: $\dot{\sigma}(t) = \mathbb{L} : [\dot{\epsilon}(t) - \dot{\epsilon}^p(t)]$ • ICs: $\sigma(0) = \mathbf{0}, \epsilon^p(0) = \mathbf{0}$
- $f(t) = \|\mathbf{s}(t)\| - s_0$
- $\mathbf{s}(t) = \text{dev}_{2D}\boldsymbol{\sigma}(t), \|\dot{\epsilon}^p\|(t) = \frac{1}{\tau} \left[\left(\frac{\|\mathbf{s}(t)\|}{s_0} \right)^{\frac{1}{\epsilon}} - 1 \right]$
- Loading: Mean constant strain rate, $\langle \epsilon \rangle(t) = t \dot{\epsilon} \mathbf{R}_\theta \cdot (\underline{e}_1 \otimes \underline{e}_1 + \alpha \underline{e}_2 \otimes \underline{e}_2) \cdot \mathbf{R}_\theta^t$
- Material properties: 2D isotropic stiffness; $\kappa_{2D} = 2\mu_{2D}, \mu_{2D} = 10^2 s_0, \epsilon = .5$
- Sources of randomness:
 - Size, aspect-ratio
orientation and position
of defects

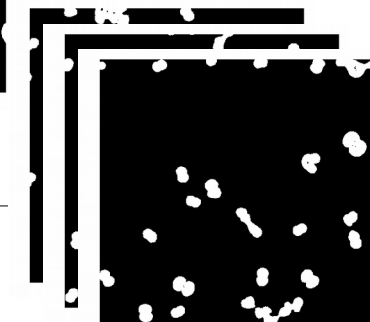
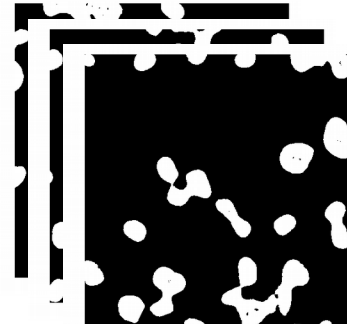
$$\dot{\epsilon}\tau = 0.1, \alpha = 1, \theta = 0$$

$$\dot{\epsilon}\tau = 1, \alpha = 1, \theta = 0$$

$$\dot{\epsilon}\tau = 10, \alpha = 1, \theta = 0$$



• Quantity of interest: Porous-plastified zone
at a given $\langle \epsilon \rangle$



Lippmann-Schwinger equation for periodic elastic media

Periodic elastic BVP:

$$\boldsymbol{\sigma}(\underline{x}) = \mathbb{L}(\underline{x}) : \boldsymbol{\varepsilon}(\underline{x}), \quad \nabla \cdot \boldsymbol{\sigma}(\underline{x}) = 0, \quad \boldsymbol{\varepsilon}(\underline{x}) = \{\nabla \underline{u}(\underline{x})\}_{sym}$$

for all $\underline{x} \in \mathbb{R}^2$, with $\mathbb{L}(\underline{x} + (n\underline{e}_1 + m\underline{e}_2)L) = \mathbb{L}(\underline{x})$ for all $n, m \in \mathbb{Z}$ s.t.

$$\underline{u}(\underline{x} + (n\underline{e}_1 + m\underline{e}_2)L) = \underline{u}(\underline{x}) + L \bar{\boldsymbol{\varepsilon}} \cdot (n\underline{e}_1 + m\underline{e}_2)$$

$$\boldsymbol{\sigma}(\underline{x} + (n\underline{e}_1 + m\underline{e}_2)) \cdot \underline{e}_k = \boldsymbol{\sigma}(\underline{x}) \cdot \underline{e}_k \text{ for } k = 1, 2$$

and where $\bar{\bullet} := \frac{1}{L^2} \int_{\Omega} \bullet(\underline{x}) d\nu_{\underline{x}}$ is a volume average over $\Omega := [0, L] \times [0, L]$.

Then, as we introduce the polarization field $\boldsymbol{\tau}$ with reference \mathbb{L}^0 ,

$$\boldsymbol{\tau}(\underline{x}) := \boldsymbol{\sigma}(\underline{x}) - \mathbb{L}^0 : \boldsymbol{\varepsilon}(\underline{x}) = \Delta \mathbb{L}(\underline{x}) : \boldsymbol{\varepsilon}(\underline{x})$$

where $\Delta \mathbb{L}(\underline{x}) := \mathbb{L}(\underline{x}) - \mathbb{L}^0$, the local statement of equilibrium becomes

$$\nabla \cdot \boldsymbol{\tau}(\underline{x}) + \nabla \cdot [\mathbb{L}^0 : \boldsymbol{\varepsilon}(\underline{x})] = 0 \quad \begin{array}{l} \text{Disturbance strain field } \tilde{\boldsymbol{\varepsilon}}(\underline{x}) \\ \text{with vanishing field average.} \end{array}$$

with solution

$$\boldsymbol{\varepsilon}(\underline{x}) = \bar{\boldsymbol{\varepsilon}} - \boxed{\boldsymbol{\Gamma} * \boldsymbol{\tau}(\underline{x})} = \bar{\boldsymbol{\varepsilon}} - \boxed{\boldsymbol{\Gamma} * [\Delta \mathbb{L} : \boldsymbol{\varepsilon}(\underline{x})]}$$

Lippmann-Schwinger equation

in which $\boldsymbol{\Gamma} * \boldsymbol{\tau}(\underline{x}) := \int_{\mathbb{R}^2} \underline{\boldsymbol{\Gamma}(\underline{x}' - \underline{x}) : \boldsymbol{\tau}(\underline{x}')} d\nu_{\underline{x}'}$. *Periodic Green operator for strains.*

Note that for all \underline{x} , we have $\bar{\boldsymbol{\varepsilon}} = [\Delta \mathbb{L}(\underline{x})]^{-1} : \boldsymbol{\tau}(\underline{x}) + \boldsymbol{\Gamma} * \boldsymbol{\tau}(\underline{x})$

Hashin-Shtrikman (HS) variational principle

Multiplying the previous expression by a test field τ' , we have

$$\tau'(\underline{x}) : \bar{\epsilon} = \tau'(\underline{x}) : [\Delta \mathbb{L}(\underline{x})]^{-1} : \tau(\underline{x}) + \tau'(\underline{x}) : (\Gamma * \tau)(\underline{x})$$

which, after volume averaging over Ω , becomes

$$\overline{\tau'} : \bar{\epsilon} = \overline{\tau' : \Delta \mathbb{L}^{-1} : \tau} + \overline{\tau' : (\Gamma * \tau)}$$

Differential of the HS functional evaluated at the equilibrated stress τ

The HS functional is defined as follows by Hashin and Shtrikman (1962):

$$\mathcal{H}(\tau') := \overline{\tau'} : \bar{\epsilon} - 1/2 \overline{\tau' : (\Delta \mathbb{L})^{-1} : \tau'} - 1/2 \overline{\tau' : (\Gamma * \tau')}$$

\mathcal{H} admits a stationary state for the equilibrated polarization field τ , irrespectively of the reference stiffness \mathbb{L}^0 . At equilibrium, we also have $\mathcal{H}(\tau) = 1/2 \bar{\epsilon} : (\mathbb{L}^{eff} - \mathbb{L}^0) : \bar{\epsilon}$, where \mathbb{L}^{eff} is s.t. $\bar{\sigma} = \mathbb{L}^{eff} : \bar{\epsilon}$.

Boundedness conditions of \mathcal{H} :

$$\Delta \mathbb{L}(\underline{x}) \text{ PSD for all } \underline{x} \text{ implies } \mathcal{V}_1 \subseteq \mathcal{V}_2 \subseteq \mathcal{V} \implies \sup_{\mathcal{V}_1} \mathcal{H} \leq \sup_{\mathcal{V}_2} \mathcal{H} \leq \sup_{\mathcal{V}} \mathcal{H} = \mathcal{H}(\tau)$$

$$\Delta \mathbb{L}(\underline{x}) \text{ NSD for all } \underline{x} \text{ implies } \mathcal{V}_1 \subseteq \mathcal{V}_2 \subseteq \mathcal{V} \implies \inf_{\mathcal{V}_1} \mathcal{H} \geq \inf_{\mathcal{V}_2} \mathcal{H} \geq \inf_{\mathcal{V}} \mathcal{H} = \mathcal{H}(\tau)$$

Searching for polarization fields among richer functional spaces guarantees not to deteriorate the quality of the solution if the reference medium is chosen properly.

Piecewise polynomial polarization fields, i.e. \mathcal{V}^{h_p}

We assume a trial polynomial field of degree p given by

$$\tau^{h_p}(\underline{x}) := \sum_{\alpha} \left(\chi_{\alpha}(\underline{x}) \boldsymbol{\tau}^{\alpha} + \chi_{\alpha}(\underline{x}) \sum_{k=1}^p \left\langle \boldsymbol{\tau}^{\alpha} \partial^k, (\underline{x} - \underline{x}^{\alpha})^{\otimes k} \right\rangle_k \right),$$

The term $\overline{\tau^{h_p} : (\Gamma * \tau^{h_p})}$ then invokes components of the form

$$\int_{\Omega_{\alpha}} \int_{\Omega_{\gamma}} (x_{r_1} - x_{r_1}^{\alpha}) \dots (x_{r_r} - x_{r_r}^{\alpha}) \Gamma_{ijkl}(\underline{x} - \underline{y}) (y_{s_1} - x_{s_1}^{\gamma}) \dots (y_{s_s} - x_{s_s}^{\gamma}) d\nu_{\underline{x}} d\nu_{\underline{y}}$$

which we reformulate by changes of variables and using a Taylor expansions of the Green operator,

$${}^n\boldsymbol{\Gamma}(\underline{x} - \underline{y} + \underline{x}_{\gamma\alpha}) := \boldsymbol{\Gamma}(\underline{x}_{\gamma\alpha}) + \sum_{k=1}^n \sum_{i=0}^k \frac{(-1)^i}{(k-i)!i!} \left\langle \boldsymbol{\Gamma}^{(k)}(\underline{x}_{\gamma\alpha}), \underline{x}^{\otimes k-i} \otimes \underline{y}^{\otimes i} \right\rangle_k \text{ for all } (\underline{x}, \underline{y}) \in \Omega'_{\alpha} \times \Omega'_{\gamma}$$

The resulting expression contains the following estimates of “r-s influence tensors of Ω_{γ} over Ω_{α} ”

$$({}^nT_{r,s}^{\alpha\gamma})_{r_1\dots r_r i j k l s_1\dots s_s} = \frac{1}{|\Omega|} [W_0^{r,0}(\Omega'_{\alpha})]_{r_1\dots r_r} \Gamma_{ijkl}(\underline{x}_{\gamma\alpha}) [W_0^{s,0}(\Omega'_{\gamma})]_{s_1\dots s_s}$$

$$+ \frac{1}{|\Omega|} \sum_{k=1}^n \sum_{i=0}^k \frac{(-1)^i}{(k-i)!i!} \Gamma_{ijklk_1\dots k_k}^{(k)}(\underline{x}_{\gamma\alpha}) [W_0^{r+k-i,0}(\Omega'_{\alpha})]_{k_1\dots k_{k-i} r_1\dots r_r} [W_0^{i+s,0}(\Omega'_{\gamma})]_{k_{k-i+1}\dots k_k s_1\dots s_s}$$

HS functional for trial fields in \mathcal{V}^{h_p} (derivation)

From our definition of the estimates of influence tensors, we obtain

$$\overline{\tau^{h_p} : n(\Gamma * \tau^{h_p})} = \sum_{\alpha} \sum_{\gamma} \left[\tau^{\alpha} : n\mathbb{T}_{0,0}^{\alpha\gamma} : \tau^{\gamma} + \sum_{r=1}^p \sum_{s=1}^p \left\langle \partial^r \tau^{\alpha}, \left\langle n\mathbb{T}_{r,s}^{\alpha\gamma}, \tau^{\gamma} \partial^s \right\rangle_{s+2} \right\rangle_{r+2} \right]$$

The other term, $\overline{\tau^{h_p} : (\Delta\mathbb{L})^{-1} : \tau^{h_p}}$ can be calculated exactly. We obtain

$$\overline{\tau^{h_p} : (\Delta\mathbb{L})^{-1} : \tau^{h_p}} = \sum_{\alpha} \Delta\mathbb{M}^{\alpha} :: \left[c_{\alpha} \tau^{\alpha} \otimes \tau^{\alpha} + \sum_{r=1}^p \sum_{s=1}^p \left\langle \tau^{\alpha} \partial^r, \left\langle \mathcal{W}_0^{r+s,0}(\Omega'_{\alpha}), \partial^s \tau^{\alpha} \right\rangle_s \right\rangle_r \right]$$

where $\Delta\mathbb{M}^{\alpha} := (\mathbb{L}^{\alpha} - \mathbb{L}^0)^{-1}$ so that the following estimate of the HS functional ${}^n\mathcal{H}(\tau^{h_p}) := \overline{\tau^{h_p} : \bar{\varepsilon}} - 1/2 \overline{\tau^{h_p} : (\Delta\mathbb{L})^{-1} : \tau^{h_p}} - 1/2 \overline{\tau^{h_p} : n(\Gamma * \tau^{h_p})}$ is

$$\begin{aligned} {}^n\mathcal{H}(\tau^{h_p}) &= \sum_{\alpha} \left(c_{\alpha} \tau^{\alpha} : \bar{\varepsilon} + \sum_{r=1}^p \left\langle \tau^{\alpha} \partial^r, \mathcal{W}_0^{r,0}(\Omega'_{\alpha}) \right\rangle_r : \bar{\varepsilon} \right) \\ &\quad - \frac{1}{2} \sum_{\alpha} \Delta\mathbb{M}^{\alpha} :: \left(c_{\alpha} \tau^{\alpha} \otimes \tau^{\alpha} + \sum_{r=1}^p \sum_{s=1}^p \left\langle \tau^{\alpha} \partial^r, \left\langle \mathcal{W}_0^{r+s,0}(\Omega'_{\alpha}), \partial^s \tau^{\alpha} \right\rangle_s \right\rangle_r \right) \\ &\quad - \frac{1}{2} \sum_{\alpha} \sum_{\gamma} \left(\tau^{\alpha} : n\mathbb{T}_{0,0}^{\alpha\gamma} : \tau^{\gamma} + \sum_{r=1}^p \sum_{s=1}^p \left\langle \partial^r \tau^{\alpha}, \left\langle n\mathbb{T}_{r,s}^{\alpha\gamma}, \tau^{\gamma} \partial^s \right\rangle_{s+2} \right\rangle_{r+2} \right) \end{aligned}$$

Stationarity conditions for trial fields in \mathcal{V}^{h_p}

The stationary state of the functional is such that

First, let $\partial_{\tau^\alpha} {}^n \mathcal{H} = \mathbf{0}$ for all α :

After using $({}^n T_{0,0}^{\gamma\alpha})_{ijkl} = ({}^n T_{0,0}^{\alpha\gamma})_{klji}$ for $\gamma \neq \alpha$ and

symmetrizing our estimates of self-influence tensors ${}^n \mathbb{T}_{0,0}^{\alpha\alpha}$, we obtain

$$c_\alpha \bar{\varepsilon} = c_\alpha \Delta \mathbb{M}^\alpha : \boldsymbol{\tau}^\alpha + \sum_\gamma {}^n \mathbb{T}_{0,0}^{\alpha\gamma} : \boldsymbol{\tau}^\gamma \quad \text{for all } \alpha.$$

Second, let $\partial_{\tau^\alpha} \partial^r {}^n \mathcal{H} = \mathbf{0}$ for all α, r s.t. $1 \leq r \leq p$:

Similarly, after using $({}^n T_{0,0}^{\gamma\alpha})_{r_1 \dots r_r i j k l s_1 \dots s_s} = ({}^n T_{0,0}^{\alpha\gamma})_{s_1 \dots s_s k l i j r_1 \dots r_r}$ for $\gamma \neq \alpha$ and
symmetrizing our estimates of self-influence tensors ${}^n \mathbb{T}_{s,r}^{\alpha\alpha}$, we obtain

$$\bar{\varepsilon} \otimes \mathcal{W}_0^{r,0}(\Omega'_\alpha) = \Delta \mathbb{M}^\alpha : \sum_{s=1}^p \left\langle \boldsymbol{\tau}^\alpha \partial^s, \mathcal{W}_0^{s+r,0}(\Omega'_\alpha) \right\rangle_s + \sum_\gamma \sum_{s=1}^p \left\langle \partial^s \boldsymbol{\tau}^\gamma, {}^n \mathbb{T}_{s,r}^{\gamma\alpha} \right\rangle_{s+2}$$

for all α, r s.t. $1 \leq r \leq p$:

“Generalized Mandel representation” for assembly of a global

We want to solve the system

$$\begin{aligned}
 r = 0 \quad & \rightarrow \{\bar{\varepsilon}^0\} = [\mathbb{D}_0^0]\{\boldsymbol{\tau}\} \\
 & \quad \begin{matrix} 3n_\alpha \times 1 & 3n_\alpha \times 3n_\alpha & 3n_\alpha \times 1 \end{matrix} \\
 r = 1 \quad & \rightarrow \{\bar{\varepsilon}^1\} = [\mathbb{D}_1^1]\{\partial\boldsymbol{\tau}\} + [\mathbb{D}_2^1]\{\partial^2\boldsymbol{\tau}\} + [\mathbb{D}_3^1]\{\partial^3\boldsymbol{\tau}\} + \cdots + [\mathbb{D}_p^1]\{\partial^p\boldsymbol{\tau}\} \\
 & \quad \begin{matrix} 6n_\alpha \times 1 & 6n_\alpha \times 6n_\alpha & 6n_\alpha \times 1 & 6n_\alpha \times 9n_\alpha & 9n_\alpha \times 1 & 6n_\alpha \times 12n_\alpha & 12n_\alpha \times 1 & 6n_\alpha \times 3(p+1)n_\alpha \end{matrix} \\
 r = 2 \quad & \rightarrow \{\bar{\varepsilon}^2\} = [\mathbb{D}_1^2]\{\partial\boldsymbol{\tau}\} + [\mathbb{D}_2^2]\{\partial^2\boldsymbol{\tau}\} + [\mathbb{D}_3^2]\{\partial^3\boldsymbol{\tau}\} + \cdots + [\mathbb{D}_p^2]\{\partial^p\boldsymbol{\tau}\} \\
 & \quad \begin{matrix} 9n_\alpha \times 1 & 9n_\alpha \times 6n_\alpha & 6n_\alpha \times 1 & 9n_\alpha \times 9n_\alpha & 9n_\alpha \times 1 & 9n_\alpha \times 12n_\alpha & 12n_\alpha \times 1 & 9n_\alpha \times 3(p+1)n_\alpha \end{matrix} \\
 r = 3 \quad & \rightarrow \{\bar{\varepsilon}^3\} = [\mathbb{D}_1^3]\{\partial\boldsymbol{\tau}\} + [\mathbb{D}_2^3]\{\partial^2\boldsymbol{\tau}\} + [\mathbb{D}_3^3]\{\partial^3\boldsymbol{\tau}\} + \cdots + [\mathbb{D}_p^3]\{\partial^p\boldsymbol{\tau}\} \\
 & \quad \begin{matrix} 12n_\alpha \times 1 & 12n_\alpha \times 6n_\alpha & 6n_\alpha \times 1 & 12n_\alpha \times 9n_\alpha & 9n_\alpha \times 1 & 12n_\alpha \times 12n_\alpha & 12n_\alpha \times 1 & 12n_\alpha \times 3(p+1)n_\alpha \end{matrix} \\
 & \quad \vdots \quad \vdots \quad \vdots \quad \vdots \quad \vdots \quad \ddots \quad \vdots \\
 & \quad \begin{matrix} 6n_\alpha \times 1 & 9n_\alpha \times 1 & 12n_\alpha \times 1 & 3(p+1)n_\alpha \times 1 \end{matrix} \\
 r = p \quad & \rightarrow \{\bar{\varepsilon}^p\} = [\mathbb{D}_1^p]\{\partial\boldsymbol{\tau}\} + [\mathbb{D}_2^p]\{\partial^2\boldsymbol{\tau}\} + [\mathbb{D}_3^p]\{\partial^3\boldsymbol{\tau}\} + \cdots + [\mathbb{D}_p^p]\{\partial^p\boldsymbol{\tau}\} \\
 & \quad \begin{matrix} 3(p+1)n_\alpha \times 1 & 3(p+1)n_\alpha \times 6n_\alpha & 3(p+1)n_\alpha \times 9n_\alpha & 3(p+1)n_\alpha \times 12n_\alpha & 3(p+1)n_\alpha \times 3(p+1)n_\alpha \end{matrix}
 \end{aligned}$$

which we recast in

$$\left\{ \begin{array}{l} \{\bar{\varepsilon}^1\} \\ \{\bar{\varepsilon}^2\} \\ \{\bar{\varepsilon}^3\} \\ \vdots \\ \{\bar{\varepsilon}^p\} \end{array} \right\} = \left[\begin{array}{ccccc} [\mathbb{D}_1^1] & [\mathbb{D}_2^1] & [\mathbb{D}_3^1] & \cdots & [\mathbb{D}_p^1] \\ [\mathbb{D}_1^2] & [\mathbb{D}_2^2] & [\mathbb{D}_3^2] & \cdots & [\mathbb{D}_p^2] \\ [\mathbb{D}_1^3] & [\mathbb{D}_2^3] & [\mathbb{D}_3^3] & \cdots & [\mathbb{D}_p^3] \\ \vdots & \vdots & \vdots & \ddots & \vdots \\ [\mathbb{D}_1^p] & [\mathbb{D}_2^p] & [\mathbb{D}_3^p] & \cdots & [\mathbb{D}_p^p] \end{array} \right] \left\{ \begin{array}{l} \{\partial\boldsymbol{\tau}\} \\ \{\partial^2\boldsymbol{\tau}\} \\ \{\partial^3\boldsymbol{\tau}\} \\ \vdots \\ \{\partial^p\boldsymbol{\tau}\} \end{array} \right\}$$

$\frac{3n_\alpha}{2}(p^2 + 3p) \times 1 \quad \frac{3n_\alpha}{2}(p^2 + 3p) \times \frac{3n_\alpha}{2}(p^2 + 3p) \quad \frac{3n_\alpha}{2}(p^2 + 3p) \times 1$

system of stationarity equations

where

$$[\mathbb{D}_s^r] := \underline{[\mathbb{M}_{s,r}]} + \overline{[\mathbb{T}_{s,r}]} \quad \boxed{\text{Assembly of components of compliances } \Delta\mathbb{M}^\alpha \text{ weighted by Minkowski tensors.}}$$

Assembly of components of self-influence and influence tensors.

2D Barnett-Lothe integral formalism

- The Green operator is obtained as follows from the Green's function,
- $$4\Gamma_{ijkl}(r, \theta) := G_{ik,jl}^{(2)}(r, \theta) + G_{il,jk}^{(2)}(r, \theta) + G_{jk,il}^{(2)}(r, \theta) + G_{jl,ik}^{(2)}(r, \theta)$$
- Irrespectively of the material symmetry, 2D Green's functions are a by-product of the Barnett-Lothe (1973) integral formalism. We have

$$2\mathbf{G}(r, \theta) = -\frac{1}{\pi} \ln(r)\mathbf{H}(\pi) - \mathbf{S}(\theta) \cdot \mathbf{H}(\pi) - \mathbf{H}(\theta) \cdot \mathbf{S}^T(\pi)$$

where $\mathbf{S}(\theta) = \frac{1}{\pi} \int_0^\theta \mathbf{N}^1(\psi) d\psi$ and $\mathbf{H}(\theta) = \frac{1}{\pi} \int_0^\theta \mathbf{N}^2(\psi) d\psi$ are incomplete Barnett-Lothe integrals with integrands readily computable for every symmetry.

- To evaluate Γ_{ijkl} , we only need those integrands and the complete integrals $\mathbf{S}(\pi)$ and $\mathbf{H}(\pi)$, which we evaluate numerically.
- We derive the following recurrence relations:

$$2\pi G_{ij,k_1 \dots k_n}^{(n)}(r, \theta) = (-r)^{-n} h_{ijk_1 \dots k_n}^n(\theta)$$

$$h_{ijk_1 \dots k_n}^n(\theta) = (n-1)h_{ijk_1 \dots k_{n-1}}^{n-1}(\theta)n_{k_n}(\theta) - \partial_\theta[h_{ijk_1 \dots k_{n-1}}^{n-1}(\theta)]m_{k_n}(\theta) \quad \text{for } n \geq 2$$

$$\partial_\theta^k[h_{ijk_1 \dots k_n}^n(\theta)] = \sum_{s=0}^k \binom{k}{s} \left\{ (n-1)\partial_\theta^{k-s}[h_{ijk_1 \dots k_{n-1}}^{n-1}(\theta)]\partial_\theta^s[n_{k_n}(\theta)] - \partial_\theta^{k-s+1}[h_{ijk_1 \dots k_{n-1}}^{n-1}(\theta)]\partial_\theta^{s+1}[n_{k_n}(\theta)] \right\}$$

$$h_{ijk_1}^1(\theta) = H_{ij}n_{k_1}(\theta) + [N_{is}^1(\theta)H_{sj} + N_{is}^2(\theta)S_{js}]m_{k_1}(\theta)$$

$$\partial_\theta^k[h_{ijk_1}^1(\theta)] = H_{ij}\partial_\theta^k[n_{k_1}(\theta)] + \sum_{s=0}^k \binom{k}{s} \left\{ H_{lj}\partial_\theta^{k-s}[N_{il}^1(\theta)] + S_{jl}\partial_\theta^{k-s}[N_{il}^2(\theta)] \right\} \partial_\theta^s[m_{k_1}(\theta)]$$

Requires evaluation of
 $\partial_\theta^k[N_{il}^1(\theta)]$ and $\partial_\theta^k[N_{il}^2(\theta)]$
for $k = 0, \dots, n-1$

2D Anisotropy

- Polar representation of 2D anisotropic stiffnesses, see Vannucci (2016)

$$L_{1111} = T_0 + 2T_1 + R_0 \cos(4\Phi_0) + 4R_1 \cos(2\Phi_1)$$

$$L_{1112} = R_0 \sin(4\Phi_0) + 2R_1 \sin(2\Phi_1)$$

$$L_{1122} = -T_0 + 2T_1 - R_0 \cos(4\Phi_0)$$

$$L_{1212} = T_0 - R_0 \cos(4\Phi_0)$$

$$L_{2212} = -R_0 \sin(4\Phi_0) + 2R_1 \sin(2\Phi_1)$$

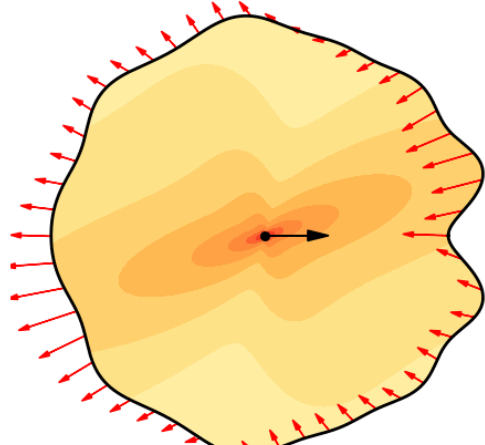
$$L_{2222} = T_0 + 2T_1 + R_0 \cos(4\Phi_0) - 4R_1 \cos(2\Phi_1)$$

T_0, T_1 : Isotropic polar invariants

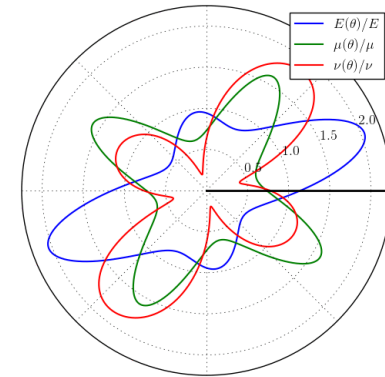
$R_0, R_1, \Phi_0 - \Phi_1$: Anisotropic polar invariants

Substitute Φ_j by $\Phi_j - \theta$ for counter clockwise positive passive rotation

Validation
Equilibrated traction fields
on random curves



Polar diagram of generalized moduli



Conditions for positive strain energy

$$T_0 - R_0 > 0,$$

$$T_1(T_0^2 - R_0^2) - 2R_1^2\{T_0 - R_0 \cos[4(\Phi_0 - \Phi_1)]\} > 0,$$

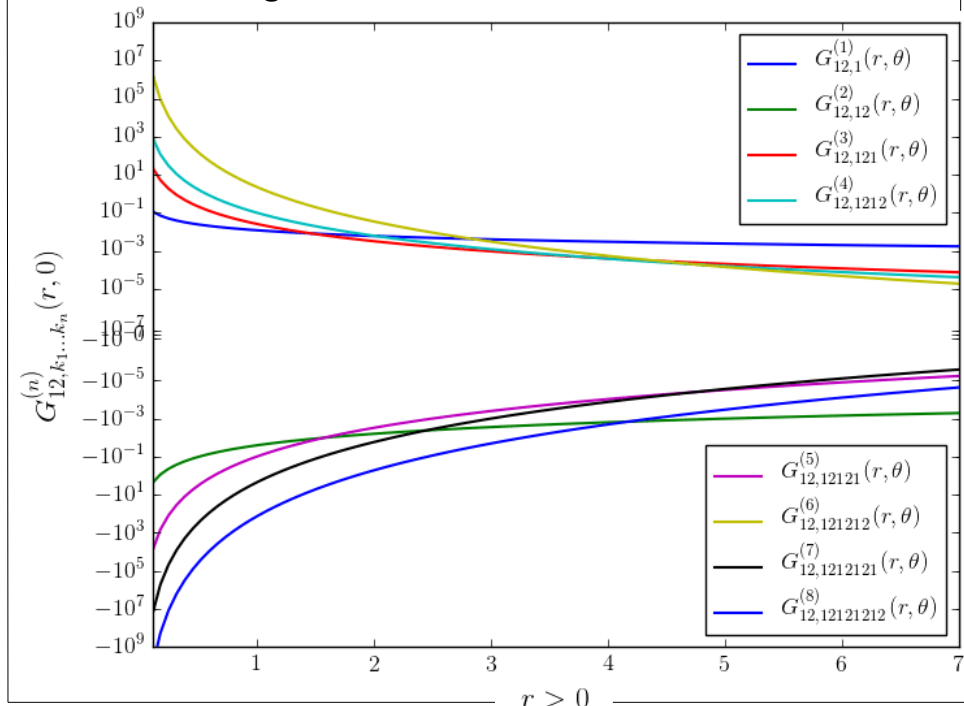
$$R_0 \geq 0,$$

$$R_1 \geq 0.$$

$$R_0 R_1^2 \sin[4(\Phi_0 - \Phi_1)] \neq 0$$

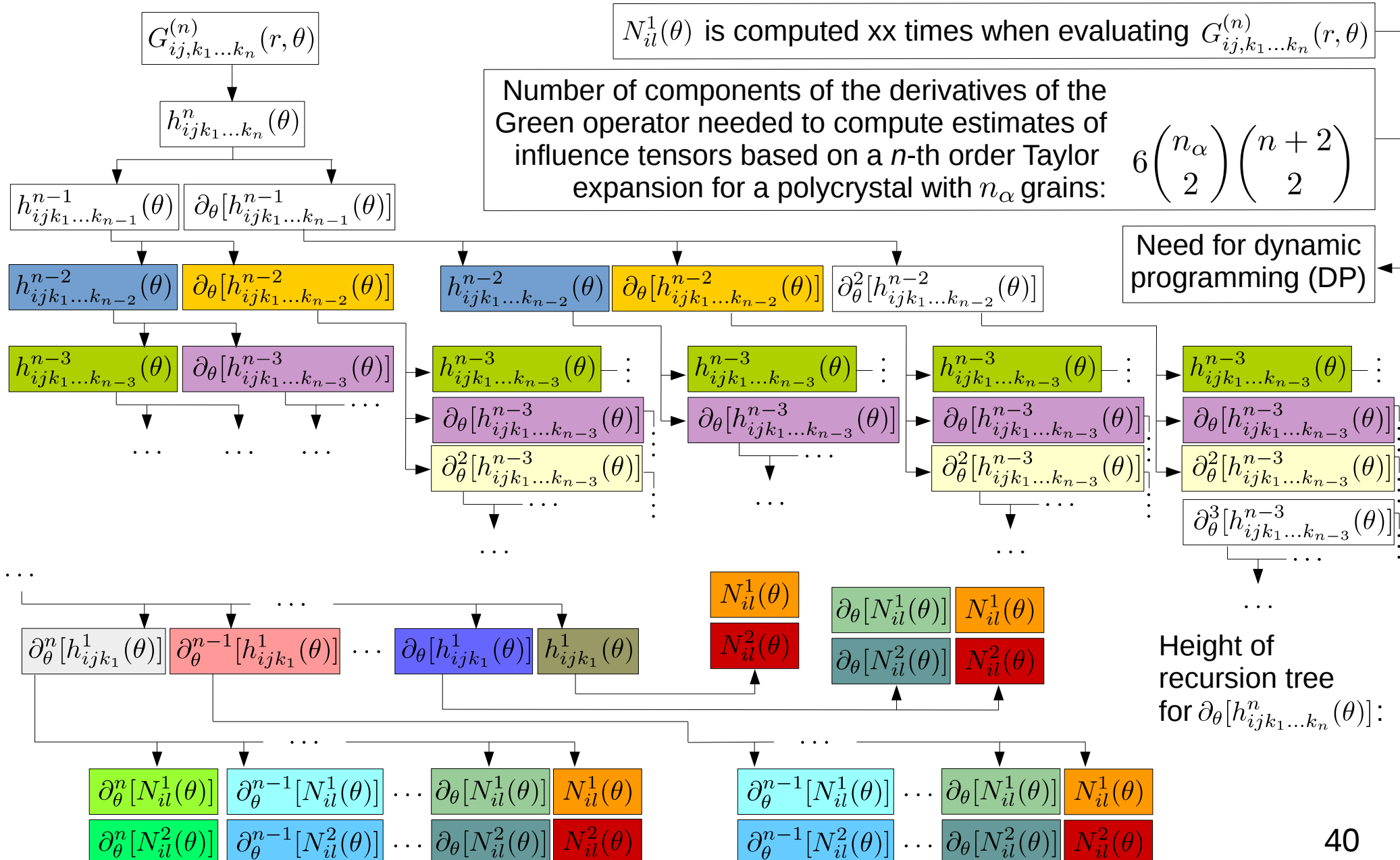
$$R_0 R_1^2 \sin[4(\Phi_0 - \Phi_1)] = 0 \implies \text{Symmetry}$$

Computed components of some gradients of the Green's function



Drawback of a simple recursive implementation

- Computing the n -th derivative of an anisotropic Green's function at a location (r, θ) leads up to the following recurrence tree:



A bottom-up DP algorithm

- We derive the following bottom-up DP algorithm to compute $h_{ijk_1 \dots k_n}^n(\theta)$:

```
def  $h_{ijk_1 \dots k_n}^n(\theta)$  :
```

```
    d0hk := zeros(n)
```

```
    for  $k \in [1, n]$  :
```

```
        for rr  $\in [0, n - k]$  :
```

```
             $r = n - k - rr$ 
```

```
            for  $s \in [0, r]$  :
```

```
                if ( $s == 0$ ) :
```

```
                    if ( $k == 1$ ) :
```

```
                        d0hk[r + k - 1] =  $H_{ij} \partial_\theta^r [n_{k_1}(\theta)] + \{H_{lj} \partial_\theta^r [N_{il}^1(\theta)] + S_{jl} \partial_\theta^r [N_{il}^2(\theta)]\} m_{k_1}(\theta)$ 
```

```
                    else :
```

```
                        d0hk[r + k - 1] =  $(k - 1)d0hk[r + k - 2]n_{k_k}(\theta) - d0hk[r + k - 1]\partial_\theta^1[n_{k_k}(\theta)]$ 
```

```
                else :
```

```
                    if ( $k == 1$ ) :
```

```
                        d0hk[r + k - 1]+ =  $\binom{r}{s} \{H_{lj} \partial_\theta^{r-s} [N_{il}^1(\theta)] + S_{jl} \partial_\theta^{r-s} [N_{il}^2(\theta)]\} \partial_\theta^s[m_{k_1}(\theta)]$ 
```

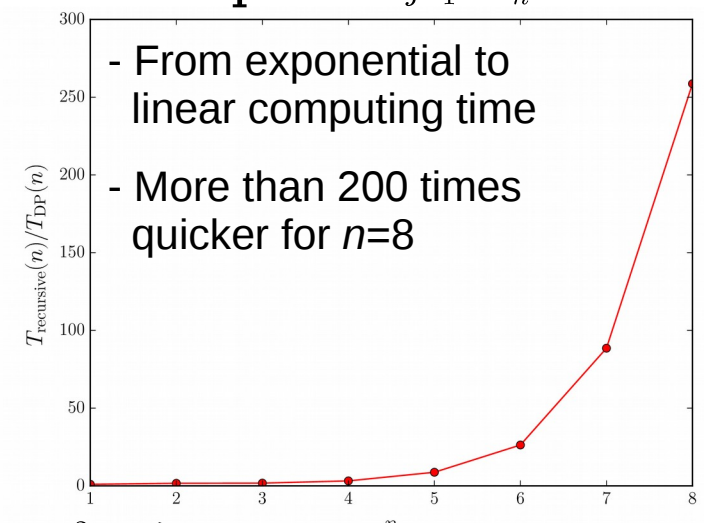
```
                    else :
```

```
                        d0hk[r + k - 1]+ =  $\binom{r}{s} \{(k - 1)d0hk[r - s + k - 2]\partial_\theta^s[n_{k_k}(\theta)] - d0hk[r - s + k - 1]\partial_\theta^{s+1}[n_{k_k}(\theta)]\}$ 
```

#At this stage, $r \in [0, n - k] \implies d0hk[r + k - 1] = \partial_\theta^r[h_{ijk_1 \dots k_k}^k(\theta)]$

#At this stage, $k \in [1, n] \implies d0hk[k - 1] = h_{ijk_1 \dots k_k}^k(\theta)$

return $d0hk[n - 1]$



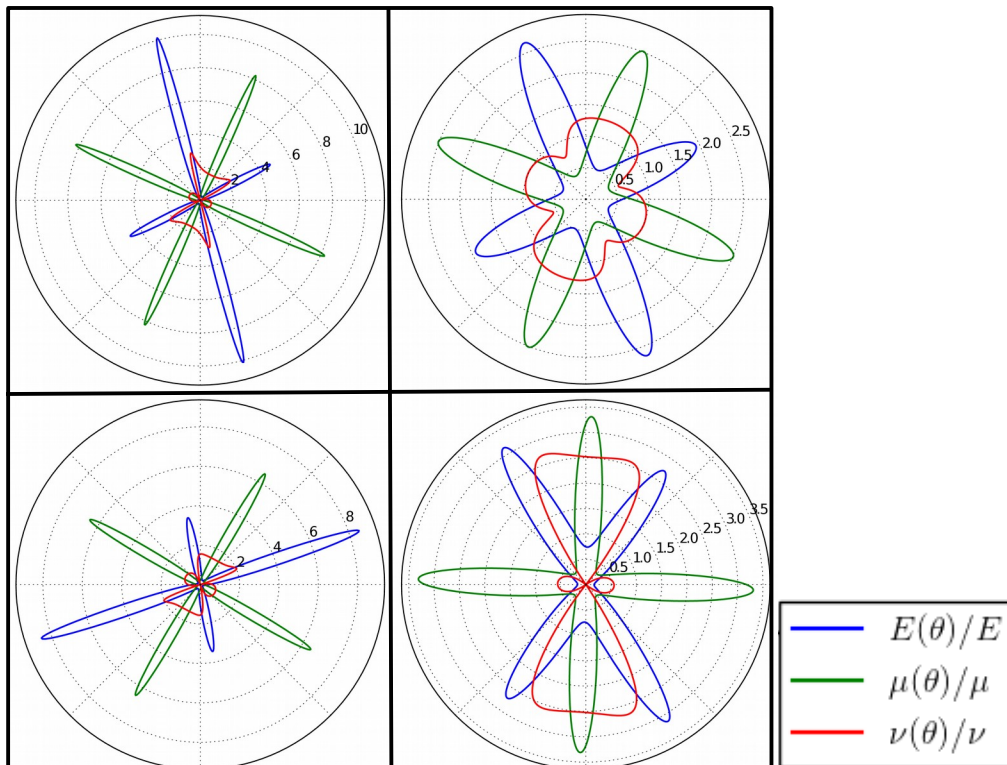
Morphological characterization for simple geometries

- As a first application, we consider a 2D periodic array of anisotropic squares. The corresponding Minkowski tensors of interest have components

$$[\mathcal{W}_0^{r,0}](n_1) := [\mathcal{W}_0^{r,0}] \underbrace{\underbrace{\dots}_{(n_1 \text{ times})}}_{11\dots 1} \underbrace{\underbrace{\dots}_{(r-n_1 \text{ times})}}_{22\dots 2}$$

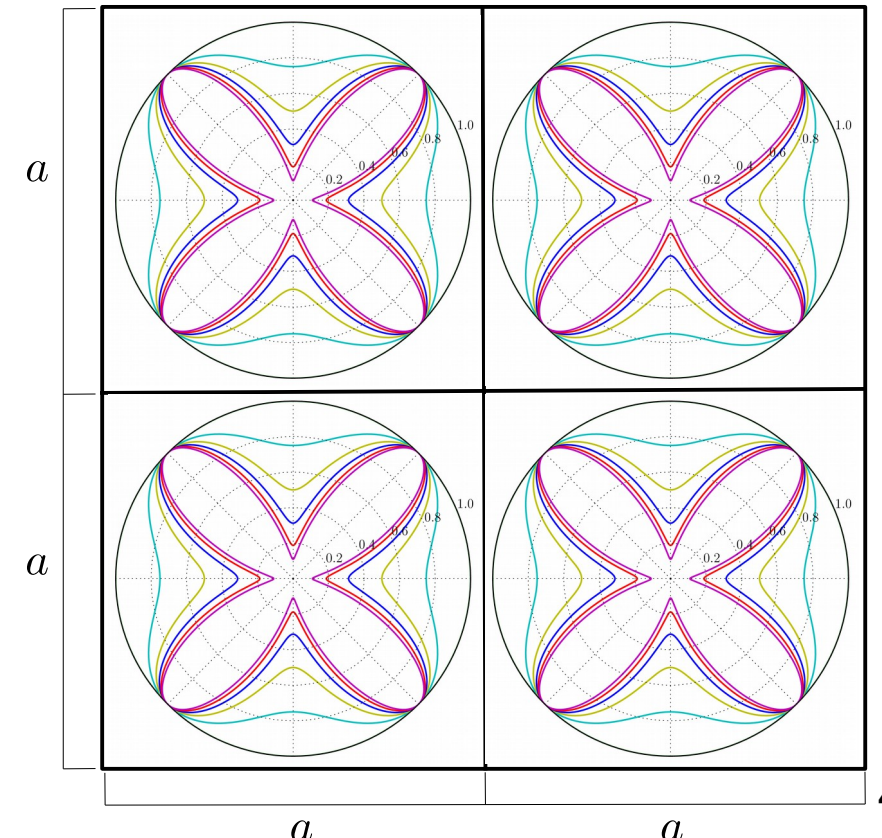
$$[\mathcal{W}_0^{r,0}](n_1) = \frac{(a/2)^{n_1+n_2+2} - (-a/2)^{n_1+1}(a/2)^{n_2+1} - (a/2)^{n_1+1}(-a/2)^{n_2+1} + (-a/2)^{n_1+1}(-a/2)^{n_2+1}}{(n_1+1)(n_2+1)}$$

Polar diagram of generalized moduli



$$\boxed{n_1 \in [0, r]} \\ n_2 := r - n_1$$

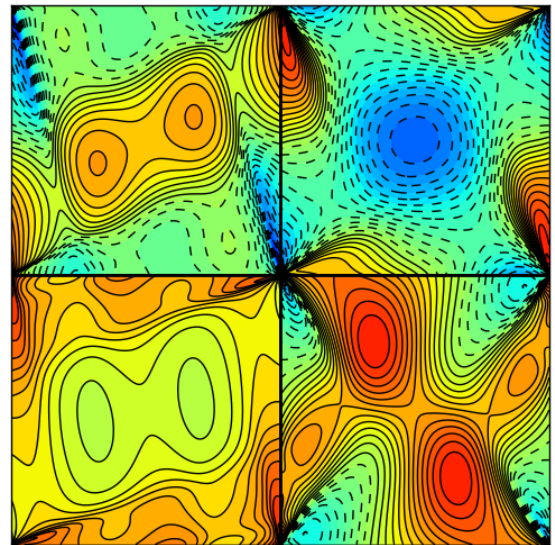
Reynolds glyphs of normalized Minkowski tensors $\mathcal{W}_0^{r,0}$ for $r \leq 12$



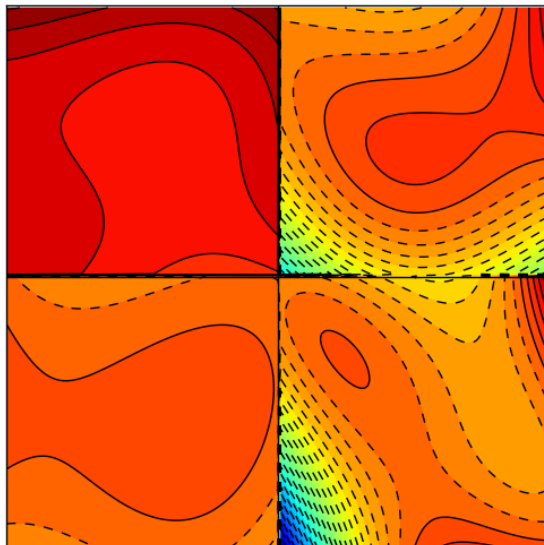
Results

- Preliminary results for a uniaxial average strain $\langle \varepsilon \rangle = \underline{e}_2 \otimes \underline{e}_2$

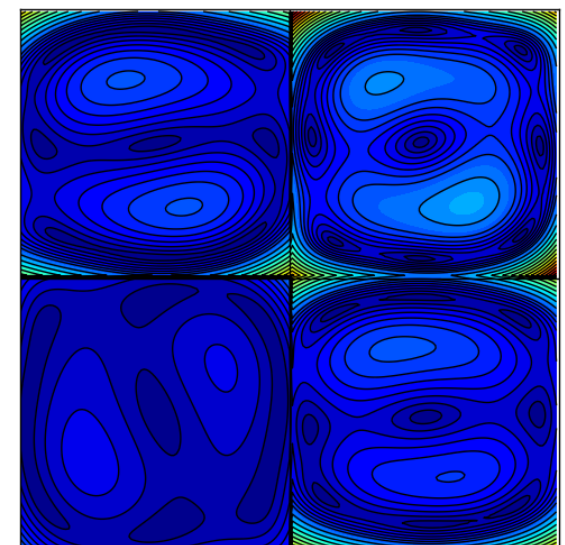
Spectral solver



Polynomial HS

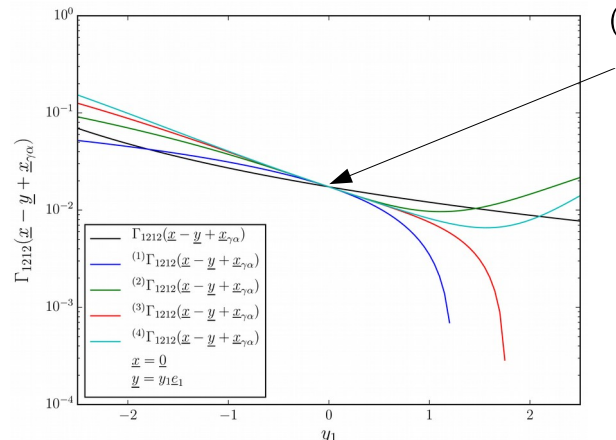


Polynomial HS



VERY POOR QUALITATIVE RESULTS

- The change of variables used to construct $(^nT_{r,s}^{\alpha\gamma})_{r_1\dots r_r i j k l s_1\dots s_s}$ requires to evaluate the Taylor expansion of the Green operator near the origin, where it is a *very bad approximation*



$(n)\Gamma_{ijkl}(x_{\gamma\alpha})$

